

STAR FORMATION IN MAGNETIC CLOUDS

TAKENORI NAKANO

Nobeyama Radio Observatory, National Astronomical Observatory, Nobeyama, Minamimaki, Minamisaku, Nagano 384-13, Japan

Received 1997 May 19; accepted 1997 September 30

ABSTRACT

This paper reexamines the widely accepted assumption that low-mass stars form mainly in magnetically subcritical cloud cores and high-mass stars form in magnetically supercritical ones. Cloud cores, as well as molecular clouds, are shown to be magnetically supercritical because although the cores are generally observed as portions of a molecular cloud having considerably higher column densities than their surroundings, magnetically subcritical condensations embedded in a cloud are not very likely to have higher column densities than their surroundings, and because it is difficult to maintain the nonthermal velocity dispersions widely observed in the cores for a significant fraction of their lifetimes if the cores are magnetically subcritical. In a magnetically supercritical condensation, which we call a core, for the pressure P_s of the surrounding medium there is a critical value P_{cr} above which the core cannot be in magnetohydrostatic equilibrium and collapses; P_{cr} depends sharply on the core mass, on the effective sound velocity in the core, which includes the effect of turbulence, and on the effective coefficient a_{eff} for the gravity diluted by magnetic force. The cloud core begins dynamical contraction when P_{cr} has decreased below P_s by some mechanism. Dissipation of turbulence is the most important process in reducing P_{cr} . Therefore, in most cases, the timescale of star formation in each core is the dissipation time of turbulence, which is several times the free-fall time of the core. For the cores of magnetic flux Φ very close to the critical flux Φ_{cr} or with small $a_{eff} \approx 1 - (\Phi/\Phi_{cr})^2$, P_{cr} will not decrease below P_s even when turbulence has completely dissipated; this will happen only in very low mass cores because of the sharp mass dependence of P_{cr} . Such cores begin dynamical contraction after a_{eff} has increased somewhat because of magnetic flux loss from their central parts by ambipolar diffusion; for this to happen, only a slight loss of magnetic flux is needed because of sharp dependence of P_{cr} on Φ at $\Phi \approx \Phi_{cr}$. The timescale of star formation in this case is not much different from the dissipation time of the turbulence, though the probability that the cores have $\Phi \approx \Phi_{cr}$ must be low. It is shown to be implausible that cloud cores form from magnetically subcritical condensations via ambipolar diffusion.

Subject headings: ISM: clouds — ISM: kinematics and dynamics — ISM: magnetic fields — MHD — stars: formation

1. INTRODUCTION

It has long been speculated that stars form in bimodal ways (see, e.g., Herbig 1970; Mezger & Smith 1977). Recently this has widely been attributed to the strength of the magnetic fields in molecular cloud cores; massive stars form in magnetically supercritical cloud cores, whose magnetic flux Φ is smaller than the critical magnetic flux Φ_{cr} (see § 2.1 for details), via dynamical contraction, and low-mass stars form mainly in magnetically subcritical cores having $\Phi > \Phi_{cr}$ that contract quasi-statically via ambipolar diffusion in the early stage and shift to dynamical contraction after their central parts become magnetically supercritical (see, e.g., Shu, Adams, & Lizano 1987; as for low-mass star formation, see also McKee 1989). Many papers have recently been published on the contraction of clouds that are initially highly magnetically subcritical (see, e.g., Fiedler & Mouschovias 1993; Ciolek & Mouschovias 1994; Basu & Mouschovias 1994; Safier, McKee, & Stahler 1997), and some observations of molecular cloud cores were compared with the results of these simulations (Crutcher et al. 1994; André, Ward-Thompson, & Motte 1996).

However, observations of magnetic fields in molecular cloud cores do not seem to fully support this assumption; although it is suggested that some cloud cores are nearly magnetically critical, others are suggested to be magnetically supercritical, and there are no cloud cores that have been confirmed to be magnetically subcritical (see § 2.4 for details).

While McKee et al. (1993) showed that molecular clouds

are magnetically supercritical, it has been uncertain whether or not cloud cores embedded in molecular clouds are magnetically supercritical. From statistical analysis and theoretical consideration of clumps embedded in molecular clouds, Bertoldi & McKee (1992) argued that the most massive clumps are magnetically supercritical, but they postponed forming a conclusion about the lower mass clumps. Thus, even theoretically, it has not yet been confirmed that some observed clumps and cores can be magnetically subcritical.

In such situations, it would be necessary to reexamine the processes of star formation in magnetic cloud cores, especially the formation of low-mass stars in magnetically supercritical cores. The purpose of this paper is to investigate the physical state of magnetic cloud cores and the processes that put the cores in magnetohydrostatic equilibrium to dynamical contraction. In § 2 we discuss whether or not the observed molecular clouds and cloud cores can be magnetically subcritical. Cloud cores are generally observed as portions of a molecular cloud whose column densities are somewhat higher than the mean column density of the cloud in which they are embedded and show nonthermal velocity dispersions (see, e.g., Myers, Linke, & Benson 1983; Myers & Benson 1983; Tatematsu et al. 1993). Our conclusion is that such cores, as well as molecular clouds themselves, are magnetically supercritical. In § 3 we investigate via the virial theorem the equilibrium state of magnetically supercritical condensations, which we call

cores, embedded in clouds and show that there is a critical surface pressure for equilibrium by considering some cases of core configuration. In § 4 we discuss the processes that can reduce the critical surface pressure and as a result induce dynamical contraction in the cores. In § 5 we investigate the physical state and evolution of magnetically subcritical condensations embedded in molecular clouds and compare our findings with those of previous works. We discuss some related problems such as formation processes of cloud cores and the timescale of star formation in § 6 and give a summary and our conclusion in § 7. In the Appendix, the results of which are used in the text, we investigate the dissipation of hydromagnetic waves and the possibility of their excitation in clouds and cloud cores.

2. ARE MOLECULAR CLOUDS AND CLOUD CORES MAGNETICALLY SUBCRITICAL?

2.1. Molecular Clouds

The virial equation for an axisymmetric oblate magnetic cloud of mass M and semimajor and semiminor axes R and Z , respectively, embedded in a medium of pressure P_s can be written as

$$\frac{1}{2} \frac{d^2 I}{dt^2} = M \left(\frac{3k_B T}{\mu m_H} + V_{\text{turb}}^2 \right) - a \frac{GM^2}{R} + b(B^2 R^3 - B_0^2 R_0^3) - 4\pi R^2 Z P_s. \quad (1)$$

Here I is the generalized moment of inertia of the cloud, t is the time, k_B , T , μ , and m_H are the Boltzmann constant, the mean temperature of the cloud, the mean molecular weight of the gas, and the mass of a hydrogen atom, respectively, V_{turb} and B are the mean turbulent velocity and the mean magnetic field strength, respectively, in the cloud, B_0 is the strength of a uniform magnetic field far from the cloud, R_0 is the radius of the magnetic tube penetrating the cloud at a place far from the cloud and satisfying

$$B_0 R_0^2 = BR^2, \quad (2)$$

a and b are dimensionless coefficients of order unity, and P_s is the pressure at the cloud surface, or equivalently the pressure of the surrounding medium. The mean direction of magnetic field has been assumed to be parallel to the minor axis. The case of $B_0 = 0$ has been investigated by many authors (see, e.g., Chandrasekhar & Fermi 1953; Mestel 1965; Strittmatter 1966), and the case of $B_0 \neq 0$ has been investigated by Nakano (1981, 1984) and McKee & Zweibel (1992). We have neglected the effect of cloud rotation in equation (1) because observations show that it is inefficient in most clouds and cloud cores (Goldsmith & Arquilla 1985; Goodman et al. 1993).

Although the magnetic field causes the cloud to be non-spherical and the tensor virial equations might be recommended, a scalar virial equation like equation (1) agrees well with the component of the tensor virial equations perpendicular to the mean direction of magnetic field (Strittmatter 1966).

We define the effective sound velocity C_{eff} , the magnetic flux Φ of the cloud, and the critical magnetic flux Φ_{cr} of the cloud, respectively, as

$$C_{\text{eff}}^2 = \frac{k_B T}{\mu m_H} + \frac{1}{3} V_{\text{turb}}^2, \quad (3)$$

$$\Phi = \pi R^2 B, \quad (4)$$

and

$$\Phi_{\text{cr}} = f_\phi G^{1/2} M, \quad (5)$$

where $f_\phi = \pi(a/b)^{1/2}$. With these quantities, equation (1) can be rewritten as

$$\frac{1}{2} \frac{d^2 I}{dt^2} = 3C_{\text{eff}}^2 M - a \frac{GM^2}{R} \left[1 - \left(\frac{\Phi}{\Phi_{\text{cr}}} \right)^2 \left(1 - \frac{R}{R_0} \right) \right] - 4\pi R^2 Z P_s. \quad (6)$$

As seen from this equation, the magnetic force in a cloud with $\Phi > \Phi_{\text{cr}}$ is stronger than the gravitational force when $R \ll R_0$ and the cloud cannot contract to a state of $R \ll R_0$ by its own gravity. Such a cloud is said to be magnetically subcritical. A cloud with $\Phi < \Phi_{\text{cr}}$ is said to be magnetically supercritical because the magnetic force is not strong enough to support the cloud. For oblate spheroidal clouds of uniform density, Strittmatter (1966) found that f_ϕ takes a value between 4.9 and 9.4 for the ratio Z/R between 1 and 0. From some numerical cloud models, Mouschovias & Spitzer (1976) obtained $f_\phi \approx 8.0$, and Tomisaka, Ikeuchi, & Nakamura (1988) found $f_\phi \approx 8.3$.

Instead of using Φ_{cr} , we can introduce the critical mean magnetic field strength of the cloud using

$$B_{\text{cr}} = f_\phi G^{1/2} \Sigma, \quad (7)$$

where $\Sigma = M/\pi R^2$ is the mean column density of the cloud along the minor axis or along the mean direction of magnetic field; the clouds with $B > B_{\text{cr}}$ and $B < B_{\text{cr}}$ are magnetically subcritical and supercritical, respectively. It is to be noted that an isothermal gaseous disk penetrated by a uniform magnetic field B perpendicular to the disk layer is gravitationally unstable only when the field B is weaker than the critical field $\tilde{B}_{\text{cr}} = 2\pi G^{1/2} \Sigma$, where Σ is the column density of the disk (Nakano & Nakamura 1978; Nakano 1988). The coefficient 2π in this expression is close to the median value of f_ϕ cited above. This condition for gravitational instability, $B < \tilde{B}_{\text{cr}}$, is almost equivalent to the necessary condition for dynamical contraction of the cloud, $B < B_{\text{cr}}$ or $\Phi < \Phi_{\text{cr}}$.

A magnetically subcritical cloud, if it exists, can be in magnetohydrostatic equilibrium only when the expansion of the cloud by magnetic force is controlled by the external pressure P_s and/or the external magnetic field B_0 . It follows from equation (6) that in virial equilibrium ($d^2 I/dt^2 = 0$), the cloud satisfies

$$P_s = C_{\text{eff}}^2 \rho + 2b \frac{B^2 R}{8\pi Z} \left[1 - \frac{R}{R_0} - \left(\frac{\Phi_{\text{cr}}}{\Phi} \right)^2 \right], \quad (8)$$

where

$$\rho = \frac{3M}{4\pi R^2 Z} \quad (9)$$

is the mean density of the cloud, and the coefficient $2b \sim 1$.

The extent to which molecular clouds can be magnetically subcritical may be estimated from the pressure of the interstellar medium acting on the cloud surface. The intercloud medium and diffuse clouds have a pressure $P/k_B \approx 10^2 - 2 \times 10^4 \text{ cm}^{-3} \text{ K}$ (Myers 1978; Cox 1988; Elmegreen 1989); the upper bound corresponds to the mag-

netic pressure for a field strength of about $8 \mu\text{G}$. For a number of molecular clouds, Myers & Goodman (1988) found magnetic field strengths ranging from $14 \mu\text{G}$ to 8mG . Because these fields are significantly stronger than the magnetic field $B_0 \sim \text{several } \mu\text{G}$ in the diffuse medium (Davies et al. 1963), we find from equation (2) that R is considerably smaller than R_0 . Because these fields have a magnetic pressure much higher than the pressure P_s of the ambient medium and because $Z \lesssim R$, we obtain $1 - (\Phi_{\text{cr}}/\Phi)^2 \approx R/R_0$, which is considerably smaller than 1, by neglecting the term $C_{\text{eff}}^2 \rho$ (compared with P_s in eq. [8]). This means that the cloud can be only slightly magnetically subcritical and that the magnetic force is mainly counteracted by self-gravity even if the internal pressure is lower than P_s . In reality, however, molecular clouds generally have an internal isotropic pressure higher than the pressure of the ambient medium (see, e.g., Myers 1978). Larson (1981) found that the internal velocity dispersion Δv is well correlated with the size L of the region and can be approximated by $\Delta v \propto L^{0.38}$ and that the density of the region $n \propto L^{-1.1}$. With these relations, we have $P \propto n(\Delta v)^2 \propto L^{-0.3}$, which decreases with the increase of the region size L . This tendency does not break down even when we adopt the modified relationships among Δv , n , and L obtained by Myers (1983) and by Dame et al. (1986). Thus, with the pressure term $C_{\text{eff}}^2 \rho > P_s$, the clouds must be magnetically supercritical.

The molecular clouds listed by Myers & Goodman (1988) have rather strong magnetic fields; their list does not contain the clouds for which only upper limits to the field strengths are known. Molecular clouds with weaker fields are magnetically supercritical as long as they have sizes and densities similar to those of the clouds listed by Myers & Goodman. Thus we can conclude that molecular clouds are magnetically supercritical.

McKee et al. (1993) also concluded that molecular clouds are magnetically supercritical with $\Phi \sim \Phi_{\text{cr}}/2$; they considered that magnetic force and nearly Alfvénic turbulence contribute almost equally to supporting molecular clouds. The analysis of Myers & Goodman (1988) shows that the clouds they listed are not far from the magnetically critical state (see also Mouschovias & Psaltis 1995). This does not contradict our conclusion, above.

2.2. Column Densities of Cloud Cores

Are the clumps and cores in molecular clouds also magnetically supercritical? On the basis of statistics on clumps and theoretical analysis, Bertoldi & McKee (1992) argued that the most massive clumps are magnetically supercritical, but they did not obtain any definite results for clumps of smaller mass.

The clumps and cores are generally observed as portions of a cloud having column densities considerably higher than the mean column density of the cloud in which they are embedded (see, e.g., Myers, Linke, & Benson 1983; Myers & Benson 1983; Tatematsu et al. 1993). We can confirm in the following way that such portions are magnetically supercritical.

Let us consider a condensation of mass M , sizes R and Z , and mean field strength B embedded in a cloud of mean field strength B_0 and pressure P_s . We assume that this condensation is in equilibrium satisfying $d^2I/dt^2 = 0$ in, e.g., equation (6). The force balance along the mean direction of magnetic field (the z -direction) also holds and can be

expressed as

$$f_\rho(C_{\text{eff}}^2 \rho - P_s) \frac{1}{Z} = a_z \frac{GM}{R^2} \rho, \quad (10)$$

where ρ is the mean density of the condensation given by equation (9), a_z is a coefficient for the gravity in the z -direction and is a quantity of order unity (only slightly larger than a for oblate condensations), and f_ρ is a correction factor for the density gradient and takes a value of several. A value of $f_\rho \approx 3$ is recommended (see § 3.1). From $d^2I/dt^2 = 0$ in equation (6) together with equations (9) and (10), we have

$$1 - \frac{R}{R_0} = \left(1 - \frac{3}{f_\rho} \frac{a_z}{a} \frac{Z}{R}\right) \left(\frac{\Phi_{\text{cr}}}{\Phi}\right)^2. \quad (11)$$

With the aid of equations (4) and (5), the column density Σ of the condensation along the mean direction of magnetic field can be given by

$$\Sigma = \frac{B}{f_\phi G^{1/2}} \frac{\Phi_{\text{cr}}}{\Phi}. \quad (12)$$

Similarly, the column density of the cloud is

$$\Sigma_0 = \frac{B_0}{f_\phi G^{1/2}} \frac{\Phi_{\text{cr}0}}{\Phi_0}. \quad (13)$$

The quantities with a subscript “0” are for the cloud except for R_0 , which is defined in equation (2). Equations (12) and (13) together with equations (2) and (11) give

$$\frac{\Sigma}{\Sigma_0} = \frac{\Phi_0}{\Phi_{\text{cr}0}} \frac{\Phi_{\text{cr}}}{\Phi} \left[1 - \left(1 - \frac{3}{f_\rho} \frac{a_z}{a} \frac{Z}{R}\right) \left(\frac{\Phi_{\text{cr}}}{\Phi}\right)^2\right]^{-2}. \quad (14)$$

For $\Phi/\Phi_{\text{cr}} \gg 1$, equation (14) gives $\Sigma/\Sigma_0 \ll 1$ because $\Phi_0/\Phi_{\text{cr}0} < 1$. For $\Phi/\Phi_{\text{cr}} = 2$, for example, we have $\Sigma/\Sigma_0 = (8/9)\Phi_0/\Phi_{\text{cr}0}$ if $R \gg Z$. For a finite value of R/Z , Σ/Σ_0 is smaller; for $R/Z = 2$, for instance, we have $\Sigma/\Sigma_0 = 0.63\Phi_0/\Phi_{\text{cr}0}$, adopting a value of $a_z/a = 1.12$ for a uniform spheroid of this shape (Binney & Tremaine 1987). In addition, McKee et al. (1993) estimate that $\Phi_0 \sim \Phi_{\text{cr}0}/2$. Thus Σ can hardly be larger than Σ_0 if $\Phi > \Phi_{\text{cr}}$. Therefore, the observed cloud cores, which have significantly higher column densities than their surroundings, are magnetically supercritical. In § 5 we shall investigate the physical state and the evolution of magnetically subcritical condensations embedded in molecular clouds.

Although we have assumed in the above discussion that the cloud cores in equilibrium are oblate, statistical considerations on observed cloud cores suggest that the cores are likely to be prolate (Myers et al. 1991; Ryden 1996). It is rather difficult to imagine prolate configurations for cores in magnetohydrostatic equilibrium. In the formation stage by, e.g., fragmentation of a filamentary cloud, the envelopes of the cores can be prolate even when the central parts are already in quasi-equilibrium and oblate (Nakamura, Hanawa, & Nakano 1995). Thus the cores in the formation stage can be prolate. Even for prolate cores in equilibrium, if they exist, equation (6) holds approximately as long as Z/R is not much larger than one.

2.3. Velocity Dispersions of Cloud Cores

There are various molecular lines from cloud cores that usually have widths much larger than their thermal widths. If the line widths originate from turbulence, the turbulence

velocity is supersonic except in cores of very small mass, and the virial mass estimated from the velocity dispersion is not much different from the mass estimated from the line intensities (see, e.g., Tatematsu et al. 1993).

Although random motion would not dissipate very rapidly if it is sub-Alfvénic, it does dissipate gradually as long as there are no sources to drive it. When the random velocity is near the virial velocity, $V_{\text{turb}} \sim (GM/R)^{1/2}$, a blob at this velocity moves a distance comparable to the core size before it stops or changes its direction of motion because any other forces are hardly stronger than the gravity in the core. Therefore, extensive mixing of matter is inevitable, and the turbulence dissipates in several times the crossing time or in several times the free-fall time of the core, $t_{\text{ff}} = (3\pi/32G\rho)^{1/2}$ (Scalo & Pumphrey 1982; Elmegreen 1985).

Somewhat regular hydromagnetic waves may exist and may contribute to the velocity dispersion (Arons & Max 1975). In molecular clouds and cloud cores, unless there are some sources to excite them, such waves also dissipate because of the friction between neutral molecules and ions on a timescale proportional to the ionization fraction (Kulsrud & Pearce 1969; Arons & Max 1975; Zweibel & Josafatsson 1983). As shown in the Appendix, the timescale of this dissipation, t_{dis} , is 0.01 times the timescale of magnetic flux loss, t_B , or less. The Appendix also shows that t_{dis} in magnetically subcritical condensations is significantly smaller than the free-fall time t_{ff} if the condensations are well shielded from interstellar ultraviolet (UV) radiation and are ionized mainly by cosmic rays.

Some sources of turbulence in a condensation, such as mass outflows from young stellar objects (YSOs), can excite hydromagnetic waves (Gammie & Ostriker 1996). For condensations without such sources, the only possibility of excitation is by disturbance from the outside. Can the hydromagnetic waves and turbulence in such condensations actually be significantly excited by disturbances from the outside? Excitation takes at least the crossing time t_{cross} of the waves across the condensation. As shown in the Appendix, t_{cross} is significantly larger than t_{dis} and the waves cannot be excited in a magnetically subcritical condensation if it is well shielded from UV radiation.

Thus, in condensations that are well shielded from UV radiation and do not contain YSOs, turbulence and hydromagnetic waves dissipate in several times the free-fall time of the condensations.

If a condensation is not well shielded from UV radiation, the ion density is much higher than in condensations shielded from UV radiation, and hydromagnetic waves may be significantly excited by disturbances from the outside, although t_{dis} is much smaller than the magnetic flux loss time t_B in any situation. As shown in the Appendix, for $t_{\text{cross}} < t_{\text{dis}}$ to hold in magnetically subcritical condensations, the ionization fraction must be more than 10^2 times higher than that in the condensations shielded from UV radiation.

The column densities of 125 cloud cores in the Orion A molecular cloud observed by Tatematsu et al. (1993) can be calculated from their masses and sizes. I found that the (geometric) mean value of the column density N_{H} is $1 \times 10^{23} \text{ cm}^{-2}$, and even the thinnest core has $N_{\text{H}} \approx 2 \times 10^{22} \text{ cm}^{-2}$. Because the masses of the cores depend on the assumed abundance of CS molecules, I also calculated N_{H} using the virial masses of the cores and found that the mean value of N_{H} is $5 \times 10^{22} \text{ cm}^{-2}$ and the thinnest core

has $N_{\text{H}} \approx 8 \times 10^{21} \text{ cm}^{-2}$, which corresponds to $A_V \approx 4.3$ mag for the ordinary grain abundance (Bohlin, Savage, & Drake 1978; Savage & Mathis 1979; see also § 4.1 below). I also found $N_{\text{H}} > 1 \times 10^{22} \text{ cm}^{-2}$ for the cores in the Taurus molecular cloud (Mizuno et al. 1994). The extinction A_λ for UV radiation is significantly larger than A_V (e.g., $A_\lambda > 3.7A_V$ for the C-ionizing radiation and $A_\lambda > 2.6A_V$ for the Mg- and Fe-ionizing radiation; Savage & Mathis 1979). Although the clumpy structure of the clouds gives less diminution of UV flux than is expected from the extinction along the line of sight (Myers & Khersonsky 1995), most of these cores cannot have an ionization fraction more than 10^2 times higher than in the cores well shielded from UV radiation.

Thus it is implausible that the ionization fraction in most cloud cores is more than 10^2 times higher than that in the cores shielded from UV radiation and that the waves can be significantly excited by disturbances from the outside. To form stars in the cores with magnetic flux Φ significantly larger than Φ_{cr} takes about an e -folding time of magnetic flux, t_B , which is at least 10 – 10^2 times t_{ff} in the cores shielded from UV radiation (see, e.g., Nishi, Nakano, & Umebayashi 1991; see also § 5.1 below). This is much larger than the dissipation times of turbulence and the waves. Therefore, if the cores without YSOs are magnetically subcritical, it is difficult to maintain the nonthermal velocity dispersions for significant fractions of their lifetimes.

Even if most cloud cores have high enough ionization fractions to satisfy $t_{\text{cross}} < t_{\text{dis}}$ and the waves are significantly excited, this inequality also requires that the flux loss time should satisfy $t_B/t_{\text{ff}} \gtrsim 300(\Phi/\Phi_{\text{cr}})$, as shown in the Appendix. Therefore, it takes at least 10^8 yr to form stars in each core of density $n_{\text{H}} \lesssim 10^5 \text{ cm}^{-3}$ if the initial flux Φ is significantly larger than Φ_{cr} . Because there is some dispersion in the initial density of the cores, there must be a dispersion of 10^8 yr or more in the formation time of stars in such cores. This requires that the dispersion in stellar age in young star clusters must be 10^8 yr or more. This seems to be too large; Cohen & Kuhn (1979) showed that the stellar age distribution in NGC 2264 has a peak at 1.6 – 3.2×10^6 yr and decreases steeply to both sides of the age, and there are only a few stars having ages exceeding 1×10^7 yr.

If the cloud cores are magnetically supercritical, the timescale of star formation in each core is nearly equal to the dissipation time of turbulence, as will be shown in § 4, and hence it is easy to maintain large velocity dispersions for significant fractions of their lifetimes.

2.4. Observations of Magnetic Fields in Cloud Cores

Crutcher et al. (1993) made OH Zeeman observations of 12 cloud cores. The only certain detection of a magnetic field was toward B1, for which the line-of-sight component of the magnetic field is not much weaker than the critical field strength. For all the other cores, only the upper bounds for the line-of-sight components, which are at least several times smaller than the critical field strengths, have been obtained. Is it possible that the magnetic fields in them are nearly perpendicular to the line of sight and that the field strengths are above the critical values? Five of these cores are in the Taurus dark cloud complex. Observational studies of linear polarizations of background and embedded stars toward the Taurus complex show that the position angle of the field in the plane of the sky varies by $\sim 60^\circ$. This suggests that the angle between the magnetic field and the

line of sight also varies by a similar amount. Therefore, it is highly implausible that the magnetic fields in all of these cores are nearly completely perpendicular to the line of sight. However, because it might be difficult to completely exclude this possibility, Crutcher et al. (1993) cautiously avoided concluding that these cores are not magnetically subcritical. On the other hand, Heiles et al. (1993) concluded that B1 is magnetically supercritical.

Crutcher et al. (1996) made CN Zeeman observations of two molecular cloud cores with negative results. The upper limits they obtained for the line-of-sight components of the magnetic fields are significantly smaller than both the critical field strengths and the strengths expected for the assumption of internal motion at the Alfvén speed, suggesting that these cores are magnetically supercritical and that the velocity dispersions in them are not caused by hydro-magnetic wave motion.

3. VIRIAL EQUILIBRIA OF CLOUD CORES

So far, no molecular cloud cores have been observationally confirmed to be magnetically subcritical. In addition, the physical considerations in §§ 2.2 and 2.3 almost completely exclude the possibility that a considerable fraction of the observed cores is magnetically subcritical. Therefore, it is worth studying the formation of even low-mass stars in magnetically supercritical cloud cores.

To extract the essence of the problem, we adopt a simple approach based on the virial equation. Because there are two parameters, R and Z , characterizing the sizes of the cloud core in equations (1) and (6), we need another equation that may give a relation between R and Z . There may be some possibilities. One possibility is to assume either that Z/R is constant because the observed molecular cloud cores are generally not highly flattened or that Z/R does not change much. Another possibility is that because the force balance along magnetic field lines is attained rather easily, we could assume that the force balance always holds in the z -direction. In the latter case, we shall find that Z/R in magnetohydrostatic equilibrium is independent of M and P_s (and hence of R) for a given value of Φ/Φ_{cr} . Thus the former case is included in the latter one as long as the equilibrium states are considered. We begin with the latter case.

3.1. Cores in Force Balance along Magnetic Field Lines

The force balance in the z -direction can be expressed by equation (10). Although we have introduced two parameters a_z and f_ρ in this equation, they appear only in the form a_z/f_ρ . Thus they can actually be regarded as a single parameter. Elimination of Z from equations (9) and (10) gives

$$\frac{\rho}{\rho_s} = 1 + \frac{3a_z GM^2}{4\pi f_\rho R^4 P_s}, \quad (15)$$

where

$$\rho_s = \frac{P_s}{C_{eff}^2} \quad (16)$$

is the density at the surface of the cloud core in pressure balance with the surrounding medium. After neglecting the term with R/R_0 in equation (6) because R is usually significantly smaller than R_0 in a magnetically supercritical cloud core (another justification for this assumption will appear at the end of § 3.1) and eliminating Z from equations (6), (9),

and (10), we have another expression for the virial equation,

$$\frac{1}{2} \frac{d^2 I}{dt^2} = 3C_{eff}^2 M \left(1 + \frac{4\pi f_\rho R^4 P_s}{3a_z GM^2} \right)^{-1} - a_{eff} \frac{GM^2}{R} \equiv F_1(R), \quad (17)$$

where

$$a_{eff} = a \left[1 - \left(\frac{\Phi}{\Phi_{cr}} \right)^2 \right] \quad (18)$$

is the coefficient for the effective gravity perpendicular to the mean direction of magnetic field (the r -direction) diluted by the magnetic force.

Figure 1 shows the virial theorem function $F_1(R)$ given by equation (17) as a function of R/R_{cr} (R_{cr} being the radius at the critical state; see eq. [20] below) for several values of P_s . The cloud core takes an equilibrium state at $F_1(R) = 0$. For fixed values of M , C_{eff} , and a_{eff} , there is a critical value $P_{cr}^{(1)}$ for the pressure of the surrounding medium, P_s , above which no equilibrium states exist. This is obtained from $F_1 = dF_1/dR = 0$ as

$$P_{cr}^{(1)} = \frac{a_z GM^2}{4\pi f_\rho R_{cr}^4} = \frac{a_z}{4\pi f_\rho a_{eff}^4 G^3 M^2} \left(\frac{9}{4} C_{eff}^2 \right)^4, \quad (19)$$

where

$$R_{cr} = \frac{4a_{eff} GM}{9C_{eff}^2}. \quad (20)$$

Equation (19) is essentially the same as equation (2.21) of Nakano (1984). For $P_s = P_{cr}^{(1)}$, there is only one equilibrium state with radius $R = R_{cr}$. For $0 < P_s < P_{cr}^{(1)}$, there are two equilibrium states for a given value of P_s . It is easily con-

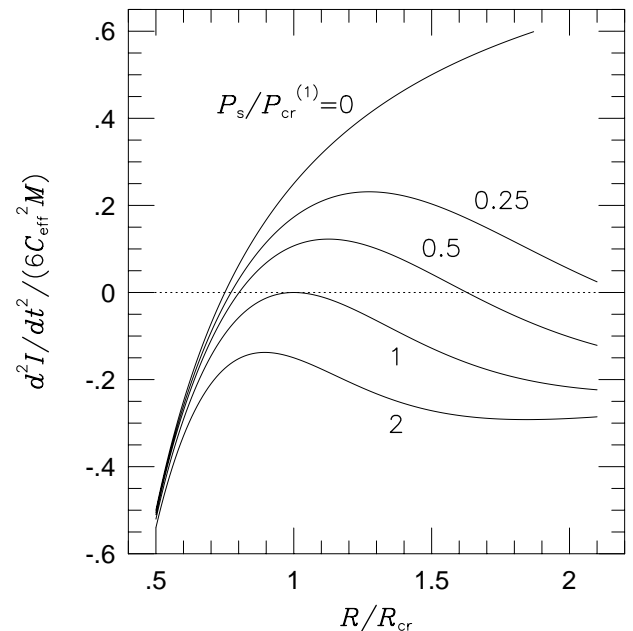


FIG. 1.—Virial theorem function for magnetically supercritical clouds in which balance holds between gravitational and pressure forces along the mean direction of magnetic field. Each curve is labeled with the surface pressure P_s in units of the critical pressure $P_{cr}^{(1)}$ given by eq. (19). The abscissa is the cloud radius R in units of the radius at the critical state R_{cr} given by eq. (20).

firmed that when the gas behaves isothermally ($C_{\text{eff}} = \text{constant}$) for perturbations, the equilibrium state with the larger radius is stable, and the one with smaller radius is unstable. When $P_s > P_{\text{cr}}^{(1)}$, we have $d^2I/dt^2 < 0$ for any R , and hence the cloud core contracts dynamically.

The radius R and the mean density ρ of the cloud core in equilibrium are determined as functions of P_s . Because these are two-valued functions, it is convenient to represent the equilibrium state through a parameter ρ/ρ_s , the density contrast of the core. Equations (15) and (20) together with $F_1(R) = 0$ in equation (17) give

$$\frac{R}{R_{\text{cr}}} = \frac{3}{4} \left(1 - \frac{\rho_s}{\rho}\right)^{-1}. \quad (21)$$

Substitution of equation (21) into equation (15) with the aid of equations (19) and (20) gives

$$\frac{P_s}{P_{\text{cr}}^{(1)}} = \frac{256}{27} \frac{\rho_s}{\rho} \left(1 - \frac{\rho_s}{\rho}\right)^3. \quad (22)$$

In the critical equilibrium state with $R = R_{\text{cr}}$ for $P_s = P_{\text{cr}}^{(1)}$, the mean density takes a critical value

$$\rho_{\text{cr}} = 4\rho_s, \quad (23)$$

as seen from equations (21) and (22). Note that if the radius and the surface pressure of the cloud core are represented in units of their critical values and the mean density in units of the density at the surface, ρ_s , the equilibrium state does not explicitly depend on the parameters M , C_{eff} , a_{eff} , a_z , and f_ρ , as seen in equations (21), (22), and (23).

From equation (10) together with equations (16), (20), and (21), we have

$$\frac{Z}{R} = \frac{f_\rho a_{\text{eff}}}{3a_z}. \quad (24)$$

This can also be obtained from equation (11) by taking $R/R_0 \ll 1$. Thus, in the equilibrium states, Z/R is a constant irrespective of M , R , and C_{eff} as long as Φ/Φ_{cr} is fixed. Without a magnetic field, or at $\Phi/\Phi_{\text{cr}} = 0$, the cloud in hydrostatic equilibrium must be spherical with $R = Z$ (we have neglected the effect of cloud rotation), and therefore $a_{\text{eff}} = a = a_z$. Thus, equation (24) recommends $f_\rho \approx 3$. Because $a_{\text{eff}} \lesssim a_z$, $Z \lesssim R$ always holds; this validates the assumption that the cloud core is oblate, which has been made in deriving the expression of the gravity term in equation (1). Equation (24) means that when $a_{\text{eff}} \sim a_z$, or when the magnetic force is not very important compared with the gravity, the cloud cores in equilibrium are not highly flattened, or $Z \sim R$, irrespective of M and C_{eff} .

In deriving equation (17) from equation (6), we have neglected the term R/R_0 compared with unity. This is a good approximation for cloud cores with $(\Phi/\Phi_{\text{cr}})^2 \ll 1$. Nearly critical cloud cores with $\Phi/\Phi_{\text{cr}} \approx 1$ may have $R \approx R_0$. If such a core is in a medium of $P_s \sim P_{\text{cr}}^{(1)}$, it contracts because equation (6) gives $d^2I/dt^2 < 0$, and it approaches a situation where $R/R_0 \ll 1$ and hence equation (17) hold. Thus equation (19) gives the critical surface pressure even for the cores with $\Phi \approx \Phi_{\text{cr}}$ as long as they are magnetically supercritical.

3.2. Cores with Fixed Z/R

So far we have assumed that the force balance holds in the z -direction between the pressure and the gravity. More simply, we may also be able to assume that Z/R is constant irrespective of R . In this case, by introducing a new

parameter,

$$f_z = \frac{Z}{R}, \quad (25)$$

we can rewrite the virial equation (6) as

$$\frac{1}{2} \frac{d^2I}{dt^2} = 3C_{\text{eff}}^2 M - a_{\text{eff}} \frac{GM^2}{R} - 4\pi R^3 P_s f_z \equiv F_2(R). \quad (26)$$

We have also neglected the term with R/R_0 . The virial theorem function $F_2(R)$ in this case is the same as those shown in Figure 1 of Nakano (1984) for nonmagnetic spherical clouds if the dimensionless coefficient a for the gravity in the abscissa is replaced with the effective coefficient a_{eff} and P_{cr} is slightly modified to $P_{\text{cr}}^{(2)}$ in equation (27) below. Although the physical states of the cores in virial equilibrium can be obtained from equation (26) in a similar way as in the above case, they can also be obtained by slightly modifying the results of the above case. We have found in the above case that Z/R in equilibrium is independent of R . We do not have the parameters a_z and f_ρ in the present case. By eliminating these parameters from equation (19) by using equations (24) and (25), we obtain the critical surface pressure in the present case,

$$P_{\text{cr}}^{(2)} = \frac{a_{\text{eff}} GM^2}{12\pi f_z R_{\text{cr}}^4} = \frac{1}{12\pi f_z a_{\text{eff}}^3 G^3 M^2} \left(\frac{9}{4} C_{\text{eff}}^2\right)^4. \quad (27)$$

The critical radius R_{cr} in this case is the same as in equation (20) because it contains neither a_z nor f_ρ . The radius R and the surface pressure P_s in the equilibrium state are given as functions of the density contrast ρ/ρ_s by equations (21) and (22), respectively, with $P_{\text{cr}}^{(2)}$ instead of $P_{\text{cr}}^{(1)}$. The mean density at the critical state in this case is also given by equation (23).

From the virial theorem for *spherical* magnetic clouds, Spitzer (1968) obtained an expression for the critical surface pressure almost the same as $P_{\text{cr}}^{(2)}$ with $f_z = 1$. By comparing the expression of Spitzer (1968) with some numerical cloud models, Mouschovias & Spitzer (1976) estimated the numerical coefficient for this expression. From the analysis of the Gibbs free energy for *spherical* magnetic clouds, Tomisaka et al. (1988) obtained the critical surface pressure similar to $P_{\text{cr}}^{(2)}$, with $f_z = 1$, and estimated the numerical coefficient for this expression by comparison with their numerical cloud models.

3.3. Comparison with Bonnor-Ebert Isothermal Spheres

The above results can be compared with the characteristics of nonmagnetic, isothermal, spherical clouds investigated by Ebert (1955) and Bonnor (1956). For the so-called Bonnor-Ebert isothermal cloud of given mass M and sound speed $C_s = (k_B T / \mu m_H)^{1/2}$, there is a critical value for the surface pressure P_s given by

$$P_{\text{cr}}^{\text{BE}} = \frac{0.685}{4\pi G^3 M^2} \left(\frac{9}{4} C_s^2\right)^4, \quad (28)$$

above which no equilibrium states exist. The cloud in equilibrium with $P_s = P_{\text{cr}}^{\text{BE}}$ has a radius

$$R_{\text{cr}}^{\text{BE}} = 0.924 \frac{4GM}{9C_s^2}. \quad (29)$$

Equation (28) is in agreement with equations (19) and (27), and equation (29) with equation (20), except for the dimensionless coefficients and the difference between C_s and C_{eff} .

For $P_s < P_{cr}^{BE}$, there is at least one equilibrium state; the number of equilibrium states depends on the value of P_s/P_{cr}^{BE} . For a given value of P_s/P_{cr}^{BE} , the equilibrium state with the lowest density contrast (central density ρ_c /density at the surface ρ_s , or mean density ρ/ρ_s) is stable, and the other equilibrium states are unstable as long as the gas behaves isothermally to perturbations. This is the same as with the characteristics of the magnetic clouds obtained above from the virial equation. The critical equilibrium state for $P_s = P_{cr}^{BE}$ has the density contrast $\rho_c/\rho_s \approx 14.0$ and $\rho/\rho_s \approx 2.46$. The latter is in fairly good agreement with the virial theorem result, $\rho_{cr}/\rho_s = 4$, shown in equation (23).

Figure 2 shows the density contrast ρ/ρ_s for the virial theorem clouds (labeled “VT”) and for the Bonnor-Ebert isothermal spheres (labeled “BE”) as a function of the surface pressure P_s ; the abscissa is normalized to the critical pressure P_{cr} , given by equations (19), (27), and (28), appropriate to each curve. The curve for virial theorem clouds has been obtained from equation (22). In both curves, the stable branches are shown as solid lines and the unstable ones as dashed lines. The curve for virial theorem clouds applies not only to magnetic clouds with force balance in the z -direction and those with $f_z = \text{constant}$ but also to non-magnetic spherical clouds that are a special case of $f_z = 1$ and $a_{eff} = a_z = a$. The differences are only in the normalization factor P_{cr} in the abscissa.

Figure 3 shows the radius of the cloud, R/R_{cr} , for the virial theorem clouds (“VT”) and for the Bonnor-Ebert isothermal spheres (“BE”) as a function of the normalized surface pressure P_s/P_{cr} . The former has been obtained from equations (21) and (22). In both curves, the stable branches are shown as solid lines and the unstable ones as dashed lines. As in Figure 2, the curve for the virial theorem clouds also applies to nonmagnetic spherical clouds.

In Figures 2 and 3, the stable branches are similar between the virial theorem clouds and the Bonnor-Ebert isothermal spheres, but the unstable branches deviate grad-

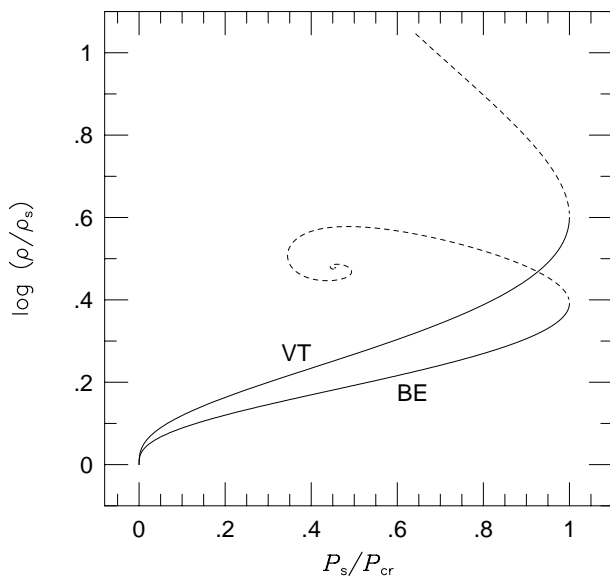


FIG. 2.—Density contrast (ratio of the mean density ρ to the density at the surface ρ_s) of the virial theorem clouds (“VT”) and the Bonnor-Ebert isothermal spheres (“BE”) as a function of the surface pressure P_s . The abscissa is normalized to the critical surface pressure P_{cr} , which is given by eqs. (19), (27), and (28). The stable branches are shown as solid lines and the unstable ones as dashed lines.

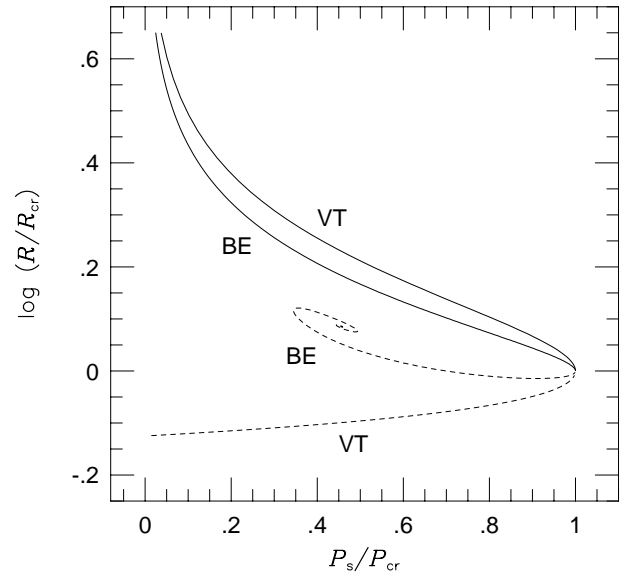


FIG. 3.—Cloud radius R as a function of the surface pressure P_s for the virial theorem clouds (“VT”) and the Bonnor-Ebert isothermal clouds (“BE”). The ordinate is normalized to the radius at the critical state R_{cr} , given by eqs. (20) and (29), and the abscissa is normalized to the critical surface pressure P_{cr} given by eqs. (19), (27), and (28). The stable branches are shown as solid lines and the unstable ones as dashed lines.

ually from each other with distance from the individual critical states at $P_s/P_{cr} = 1$. The isothermal sphere approaches a self-similar structure with density $\propto r^{-2}$, where r is the distance from the center, and spirals into a point ($P_s/P_{cr} \approx 0.455$, $\rho/\rho_s = 3.0$) in Figure 2 and a point ($P_s/P_{cr} \approx 0.455$, $R/R_{cr} \approx 1.22$) in Figure 3. The virial theorem cannot describe such detailed structure that does not have any characteristic length scale. However, the virial theorem can give good results not only for the stable states but also for the unstable states not very far from the critical state.

4. ONSET OF DYNAMICAL CONTRACTION

4.1. Critical Pressure and Ambient Pressure

The critical surface pressures $P_{cr}^{(1)}$ and $P_{cr}^{(2)}$ given by equations (19) and (27), respectively, can be rewritten numerically as

$$\frac{P_{cr}^{(1)}}{k_B} = 2.7 \times 10^5 \frac{a_z}{a_{eff}^4} \left(\frac{3}{f_\rho} \right) \left(\frac{10 M_\odot}{M} \right)^2 \times \left(\frac{C_{eff}}{0.4 \text{ km s}^{-1}} \right)^8 \text{ cm}^{-3} \text{ K} \quad (30)$$

and

$$\frac{P_{cr}^{(2)}}{k_B} = 2.7 \times 10^5 \frac{1}{a_{eff}^3} \left(\frac{1}{f_z} \right) \left(\frac{10 M_\odot}{M} \right)^2 \times \left(\frac{C_{eff}}{0.4 \text{ km s}^{-1}} \right)^8 \text{ cm}^{-3} \text{ K}. \quad (31)$$

Although one may imagine that P_{cr} decreases steeply with the core mass in proportion to M^{-2} , the observations show that the internal velocity dispersion of a cloud core tends to increase with the core mass. Tatematsu et al. (1993) found that for 125 cloud cores in the Orion A molecular cloud, the width (FWHM) of the CS ($J = 1-0$) line can be approx-

imated as $\Delta v = 0.43(M/1 M_\odot)^{0.23} \text{ km s}^{-1}$ for the core mass M , estimated from the CS line intensity, between about 10 and $2 \times 10^3 M_\odot$; the internal velocity dispersion of the cores is distributed within a factor of ~ 2 around this relationship. Bally et al. (1987) obtained a similar relationship $\Delta v = 0.54(M/1 M_\odot)^{0.25} \text{ km s}^{-1}$ for 15 ^{13}CO clumps in the Orion molecular cloud with M between about 20 and $2 \times 10^3 M_\odot$, which are larger in size and less dense than the cores described by Tatematsu et al. (1993). Larson (1981) also found a relation $\Delta v = 0.57(M/M_\odot)^{0.20} \text{ km s}^{-1}$ for a large variety of regions. With the line width (FWHM) Δv of a molecule whose mass is much larger than that of an H_2 molecule, the effective sound velocity is given by

$$C_{\text{eff}} = \left[C_s^2 + \frac{(\Delta v)^2}{8 \ln 2} \right]^{1/2}, \quad (32)$$

with the isothermal sound velocity $C_s = 0.19(T/10 \text{ K})^{1/2}(2.3/\mu)^{1/2} \text{ km s}^{-1}$.

Figure 4 shows the critical surface pressure $P_{\text{cr}}^{(1)}$ given by equations (19) and (30) as a function of the core mass M . The solid lines are for C_{eff} with the mean turbulent velocity Δv obtained by Tatematsu et al. (1993) for the cores in Orion A and cited above for the two cases of the temperature $T = 10$ and 20 K . The dashed lines are for the cases with $\Delta v = 0$. The cloud cores that have internal velocity dispersions 2 times larger than the above relationship have $P_{\text{cr}}^{(1)}$ 2.5 orders of magnitude higher than that shown in Figure 4 except at very small M . With the above empirical relation for Δv , $P_{\text{cr}}^{(1)}$ depends only slightly on M at $M \gg 10 M_\odot$, where $C_{\text{eff}}^2 \gg C_s^2$. Figure 4 also holds exactly when the ordinate is replaced with $P_{\text{cr}}^{(2)}/(k_B/a_{\text{eff}}^3 f_z)$.

It is important to estimate the pressure P_s of the medium in which cloud cores are embedded. The column density N_{H} (by number of Hydrogen nuclei) is proportional to the color excess $E(B-V)$ by $N_{\text{H}}/E(B-V) \approx 5.8 \times 10^{21} \text{ cm}^{-2} \text{ mag}^{-1}$

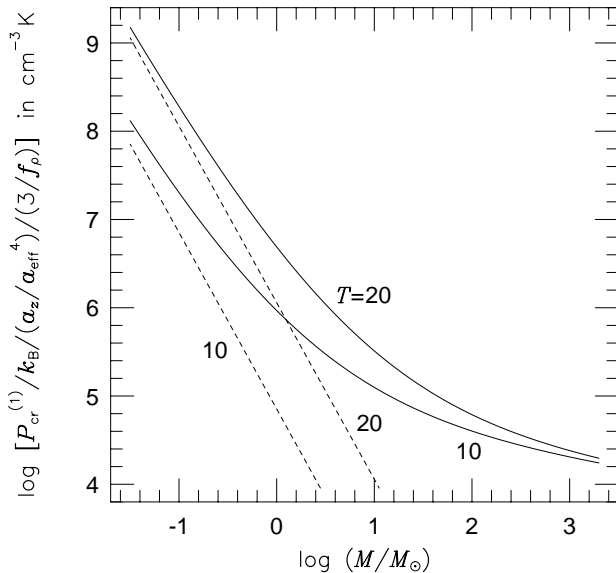


FIG. 4.—Critical surface pressure $P_{\text{cr}}^{(1)}$ given by eqs. (19) and (30) as a function of the core mass M . The solid lines are for C_{eff} with the mean turbulent velocity $\Delta v = 0.43(M/1 M_\odot)^{0.23} \text{ km s}^{-1}$ obtained for the cloud cores in the Orion A molecular cloud (Tatematsu et al. 1993) for the two cases of the temperature $T = 10$ and 20 K . The dashed lines are without turbulence for the cases of $T = 10$ and 20 K . This figure also holds exactly when the ordinate is replaced with $P_{\text{cr}}^{(2)}/(k_B/a_{\text{eff}}^3 f_z)$, which is given by eqs. (27) and (31).

(Bohlin et al. 1978). With a standard relation $A_V \approx 3.1E(B-V)$ (see, e.g., Savage & Mathis 1979) we have the column density by mass $\Sigma_0 \approx 0.0043 A_V \text{ g cm}^{-2}$ for the mass fraction of hydrogen, 0.73. Therefore, a cloud of visual extinction A_V in virial equilibrium has a mean internal pressure P_s (the surface pressure on the embedded cores unless they are located near the cloud surface) given by

$$\frac{P_s}{k_B} \approx \frac{G\Sigma_0^2}{k_B} \approx 8.0 \times 10^4 \left(\frac{A_V}{3 \text{ mag}} \right)^2 \text{ cm}^{-3} \text{ K}. \quad (33)$$

Because the ^{13}CO clumps identified in the Orion molecular cloud by Bally et al. (1987) are significantly larger and less dense than the cloud cores in Orion A identified by Tatematsu et al. (1993), some of the cores may be embedded in these clumps. From the masses, sizes, and internal velocity dispersions of the clumps, we estimate the pressure in the clumps to be $P_s/k_B \approx 10^4\text{--}10^6 \text{ cm}^{-3} \text{ K}$ except in the clump containing BN/KL and in the clump close to this, which have higher pressure enhanced probably by the activities of the young massive stars.

Comparing the curves in Figure 4 with equation (33) and the internal pressures of the Bally et al. (1987) clumps mentioned above and considering that some cloud cores have Δv somewhat larger or smaller than those given by the above relationship, we infer that a significant fraction of the cloud cores in Orion A are in magnetohydrostatic equilibrium with $P_s < P_{\text{cr}}$ and that others are contracting dynamically with $P_s > P_{\text{cr}}$.

The existence of the critical surface pressure suggests that there are several processes that can put the cloud cores in equilibrium to dynamical contraction. For example, when the pressure P_s of the medium around a cloud core is enhanced above the critical value P_{cr} by passage of shock waves, disturbances by the activities of newly born stars in the vicinity, etc., the cloud core begins to contract dynamically. In this way, so-called induced star formation occurs in the cloud cores. The expression P_{cr} also suggests some processes that can lead the cores to spontaneous star formation, which we shall discuss in the following subsections.

4.2. Dissipation of Turbulence and Waves

Equations (19) and (27) show that P_{cr} is very sensitive to C_{eff} . Many molecular cloud cores show the line widths of various molecular lines that correspond to the random velocities not very far from the virial velocity. Such random motion is usually supersonic except in cores of very small masses and is interpreted as turbulence and/or hydromagnetic wave motion. Turbulence in cloud cores dissipates in several times the free-fall time of the cores if there are no sources to drive it (Scalo & Pumphrey 1982; Elmegreen 1985). Hydromagnetic waves also dissipate because of the friction between neutral molecules and ions (Kulsrud & Pearce 1969; Arons & Max 1975; Zweibel & Josafatsson 1983). As shown in the Appendix, the dissipation time t_{dis} of the waves in cloud cores is smaller than the free-fall time if the cores are well shielded from the interstellar UV radiation and ionized mainly by cosmic rays unless $(\Phi/\Phi_{\text{cr}})^2 \ll 1$. To excite the hydromagnetic waves and turbulence by disturbances from the outside takes at least the crossing time of the waves, t_{cross} , across the core. As shown in the Appendix, unless $(\Phi/\Phi_{\text{cr}})^2 \ll 1$, t_{cross} is significantly larger than t_{dis} and the waves cannot be excited if the core is shielded from UV radiation; for the waves to be excited, or

for $t_{\text{cross}} < t_{\text{dis}}$ to hold, the ionization fraction must be more than 10^2 times higher than in the cores shielded from UV radiation. If $(\Phi/\Phi_{\text{cr}})^2 \ll 1$, the wave motion must be supersonic and super-Alfvénic, and shock dissipation must occur on a timescale much shorter than the ordinary dissipation time of the waves, t_{dis} . Therefore, such waves would not be excited even in the cores with $(\Phi/\Phi_{\text{cr}})^2 \ll 1$.

As shown in § 2.3, most of the cloud cores in the Orion A (Tatematsu et al. 1993) and Taurus (Mizuno et al. 1994) molecular clouds are thick enough to be relatively well shielded from UV radiation. Thus it is implausible that many cloud cores have ionization fractions more than 10^2 times higher than those of the cores shielded from UV radiation. Therefore, in most cloud cores, C_{eff} and, hence, P_{cr} decrease with time because no sources to drive turbulence exist before protostars form in them. When P_{cr} becomes smaller than the pressure P_s of the surrounding medium, the core begins collapsing. In this way, spontaneous star formation occurs. The time required for this type of star formation is therefore the dissipation time of the turbulence, which is several times the free-fall time of the cloud core.

Because the critical surface pressure P_{cr} is proportional to M^{-2} and the turbulence tends to have a higher fractional contribution to C_{eff} in the cores of larger M , cloud cores of higher mass can begin dynamical collapse in an earlier stage of turbulence dissipation; cores of lower mass must dissipate the turbulence to a higher degree before they begin dynamical contraction.

4.3. Magnetic Flux Loss

Cores of very small mass may not be able to begin dynamical contraction even when turbulence has completely dissipated if they have a very small a_{eff} or have Φ very close to Φ_{cr} . Such a core in magnetohydrostatic equilibrium can lose magnetic flux mainly from its central part by ambipolar diffusion (Mestel & Spitzer 1956). By magnetic flux loss, a_{eff} in the central part of the core increases, and as a result P_{cr} decreases according to equations (19) and (27). Finally, when P_{cr} falls to the pressure of the surrounding medium P_s , the core begins to collapse. This may be another way of spontaneous star formation. Because the e -folding time of magnetic flux by this process, t_B , is larger than $10t_{\text{ff}}$ in cloud cores of ordinary density (see, e.g., Nishi et al. 1991; see also § 5.1 below), the contraction of magnetically *subcritical* condensations induced by ambipolar diffusion proceeds quasi-statically and takes a time $\approx t_B$, as found by many authors (Nakano 1979, 1982, 1983, 1984; Lizano & Shu 1989; Tomisaka, Ikeuchi, & Nakamura 1990; Fiedler & Mouschovias 1993; Ciolek & Mouschovias 1994; Basu & Mouschovias 1994; Safier et al. 1997). In contrast, in magnetically *supercritical* condensations, only a slight loss of magnetic flux is required to decrease P_{cr} to P_s because P_{cr} depends sharply on Φ around $\Phi \approx \Phi_{\text{cr}}$. The time required for this is therefore much smaller than t_B and hence is not much longer than the free-fall time if the cores are shielded from UV radiation. Therefore, the time required for star formation in such cores would not be much different from the dissipation time of the initial turbulence.

However, the decrease of a_{eff} is efficient only when Φ is initially very close to Φ_{cr} . The probability that $1 - (\Phi/\Phi_{\text{cr}})^2 \ll 1$ might be very low, as suggested by the discussion on the condensations in molecular clouds in § 2.2.

There is an upper bound to a_{eff} ; at $\Phi/\Phi_{\text{cr}} < \frac{1}{2}$, it does not deviate much from the limiting value at $\Phi/\Phi_{\text{cr}} \ll 1$, as seen from equation (18). Therefore, cores of extremely small mass may not be able to contract dynamically even when the turbulence has been dissipated and the magnetic flux has decreased far below Φ_{cr} . Such cores cannot begin dynamical contraction unless, by some mechanism, the external pressure rises above the rather high critical pressure P_{cr} .

4.4. Contraction Due to Dissipation of Turbulence and Waves

As turbulence and hydromagnetic waves in the core dissipate, P_s/P_{cr} increases (assuming that the external pressure P_s is kept constant). As a result, the density contrast ρ/ρ_s increases according to equation (22) and along the solid line labeled “VT” in Figure 2, and hence R/R_{cr} decreases according to equation (21) along the solid line VT in Figure 3. Because ρ_s increases as C_{eff} decreases, as seen from equation (16), the increase of ρ is more remarkable than the increase of ρ/ρ_s . Although R_{cr} increases as turbulence and waves dissipate, as equation (20) shows, R decreases, as seen from the increase of the mean density ρ ; Z/R is kept constant as can be confirmed from equation (24) because a_{eff} is insensitive to Φ unless $\Phi \approx \Phi_{\text{cr}}$ and Φ hardly changes in the dissipation time of turbulence. Finally, when P_{cr} falls to P_s , the core begins to collapse.

Figure 5 shows this process of contraction. The abscissa is the effective sound velocity C_{eff} normalized to the effective sound velocity $C_{\text{eff}}^{\text{col}}$ at the stage when the core begins to collapse, when P_{cr} has decreased to P_s . The solid line shows

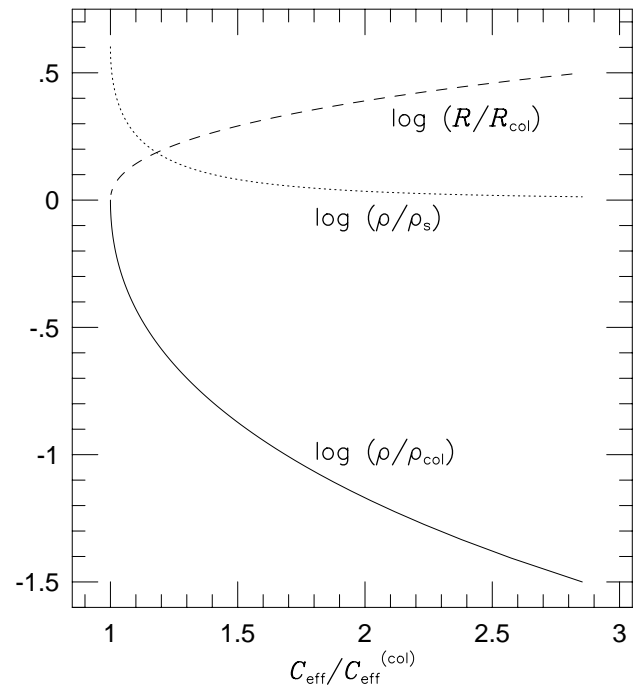


FIG. 5.—Contraction of the cloud cores induced by dissipation of turbulence up to the stage when the cores begin dynamical contraction, when the critical surface pressure P_{cr} falls to the external pressure P_s acting on the core surface. The abscissa is the effective sound velocity C_{eff} normalized to the effective sound velocity $C_{\text{eff}}^{\text{col}}$ at the stage when the cores begin to collapse and $P_{\text{cr}} = P_s$ holds. The solid line shows the variation of the mean density of the core ρ normalized to the mean density ρ_{col} at the stage at which $P_{\text{cr}} = P_s$. The dotted line is the variation of ρ/ρ_s . The dashed line shows the variation of the core radius R normalized to the radius R_{col} at the stage at which $P_{\text{cr}} = P_s$.

the mean density of the core, ρ , normalized to the mean density ρ_{col} at the stage when the core begins collapsing. The dashed line shows the radius R of the core normalized to the radius R_{col} at the stage at which $P_{\text{cr}} = P_s$. The dotted line shows ρ/ρ_s . A cloud core that initially has $C_{\text{eff}} = 2C_{\text{eff}}^{\text{col}}$ for example, must increase its mean density by a factor of 15 and decrease its radius by a factor of 2.5 before it begins collapsing.

From the observations of the cloud cores in the Taurus molecular cloud, Mizuno et al. (1994) found that the cores associated with *IRAS* sources tend to have mean densities an order of magnitude higher and radii a factor of ~ 3 smaller than do the cores without *IRAS* sources. It is to be noted that these density and radius contrasts between the two groups of cores are consistent with the results described above and shown in Figure 5; even if the central part of a core is collapsing, the size and the mean density of the core must not change much and must be nearly equal to those it had when it began collapsing. The average line width of the cores with *IRAS* sources is larger by 30% than that of the cores without *IRAS* emission (Mizuno et al. 1994). The line widths of the cores with *IRAS* sources may have been enhanced by the dynamical contraction of their central parts (M. Hayashi 1997, private communication) or by bipolar outflows from the embedded young stellar objects, despite the dissipation of the initial turbulence.

5. MAGNETICALLY SUBCRITICAL CONDENSATIONS IN CLOUDS

We confirmed in § 2 that the observed cloud cores are magnetically supercritical and investigated in §§ 3 and 4 the equilibrium states of such cores and the processes of star formation in them. On the other hand, it is not easy to deny the existence of magnetically subcritical condensations embedded in molecular clouds. If they exist, their column density Σ can hardly be higher than the column density of the cloud, Σ_0 , as shown in § 2.2. Therefore, it may be difficult to observe them unless we use the lines of the molecules that can be significantly excited in them but not as excited in the ambient medium. In this section, we investigate the evolution of magnetically subcritical condensations embedded in molecular clouds.

5.1. Evolution of Magnetically Subcritical Condensations in Molecular Clouds

Because the medium in which the condensations are embedded has a pressure $P_s \approx G\Sigma_0^2$ determined from the equilibrium condition of the cloud unless they are located near the cloud surface, and because $\Sigma \approx M/\pi R^2 \approx 2\rho Z$, equation (10) gives

$$C_{\text{eff}}^2 \rho \approx P_s + \frac{\pi a_z}{2f_\rho} G\Sigma^2 \approx P_s \left[1 + \frac{\pi a_z}{2f_\rho} \left(\frac{\Sigma}{\Sigma_0} \right)^2 \right]. \quad (34)$$

Thus the condensations with $\Sigma^2 \ll \Sigma_0^2$ are confined by pressure and have almost uniform density as long as C_{eff} is uniform in each condensation. If we consider the effect of external pressure on the molecular cloud, P_s is somewhat higher and the condensations are more highly confined by pressure. Such condensations may grow (enhance Σ) by ambipolar diffusion (Mestel & Spitzer 1956). In this growth, the density is kept constant as long as Σ is considerably smaller than Σ_0 , and therefore the growth is the change of the shape, decreasing R and increasing Z , i.e., decreasing the degree of oblateness R/Z . As seen from equations (2) and

(11), the field strength B in the condensation is nearly equal to the field strength B_0 in the cloud as long as Φ is somewhat larger than Φ_{cr} .

We estimate the timescale of such growth due to ambipolar diffusion. For any cloud configuration with whatever charged particles (various ions, electrons, and grains of various size and charge) are contained in the cloud and whatever the strength of their coupling with the cloud's magnetic field, the drift velocity of magnetic field is parallel to the magnetic force (Nakano 1984; Nakano & Umebayashi 1986). The term with $(\Phi/\Phi_{\text{cr}})^2(1 - R/R_0)$ in equation (6) corresponds to the magnetic force. In an equilibrium state, the magnetic force per unit volume can be rewritten in terms of the other forces as

$$F_{\text{mag}} \approx \frac{aGM}{R^2} \rho \left(1 - \frac{3}{f_\rho} \frac{a_z}{a} \frac{Z}{R} \right) \quad (35)$$

with the aid of equations (9) and (10); the first term on the right-hand side of the equation is the gravitational force, and the second term is the pressure force corrected for the surface pressure.

For the moment, we consider only the ion-neutral collisions as a source of the frictional force between neutral and charged particles. When the ions are nearly completely frozen in to the magnetic field as is the case in molecular clouds of ordinary density, the frictional force per unit volume is given by

$$F_{\text{fric}} \approx n_i n_n \langle \sigma v \rangle m_n v_B, \quad (36)$$

where n_i and n_n are number densities of ions and neutral gas particles, respectively, $m_n = \mu m_H$ is the mean mass of neutral gas particles, $\langle \sigma v \rangle \approx 1.5 \times 10^{-9} \text{ cm}^3 \text{ s}^{-1}$ is the collision rate coefficient for molecular gas of cosmic abundances averaged for the velocity distribution of colliding particles (Nakano 1984), and v_B is the drift velocity of the magnetic field relative to the neutrals. In equation (36), we have assumed that the mean mass m_i of the ions is much larger than m_n , as is usually the case in molecular clouds. Because we can regard that the ions drift at their terminal velocity, by equating F_{mag} and F_{fric} we have

$$v_B \approx V_B \left(1 - \frac{3}{f_\rho} \frac{a_z}{a} \frac{Z}{R} \right), \quad (37)$$

where $V_B = aGM/(R^2 n_i \langle \sigma v \rangle)$. We have chosen $n_n m_n = \rho$ because of the low ionization fraction.

When we take into account the interaction of charged grains with the magnetic field and the frictional force between charged grains and neutral gas particles, the expression for V_B in equation (37) is modified. This modification is complicated because charged grains are not always strongly coupled with magnetic field. Taking into account the effect of incompleteness of the freezing of even ions and electrons to magnetic field, Nakano (1984) and Nakano & Umebayashi (1986) obtained a general expression

$$V_B = \frac{A_1}{A} \frac{aG\rho}{R^2}, \quad (38)$$

where $A = A_1^2 + A_2^2$, $A_1 = \Sigma_v(\rho_v \omega_v^2/\tau_v \Omega_v^2)$, $A_2 = \Sigma_v(\rho_v \omega_v/\tau_v^2 \Omega_v^2)$, $\Omega_v^2 = \omega_v^2 + \tau_v^{-2}$, and ρ_v , ω_v , and τ_v are the mass density, cyclotron frequency, and viscous damping time, respectively, of charged particle v . When ions are frozen in to the magnetic field ($\tau_i \omega_i \gg 1$) and the contribution of charged grains in connecting the magnetic field with

the neutral gas particles is negligible compared with that of ions (because of, e.g., a significantly high ionization fraction and a weak magnetic field with $|\tau_g \omega_g| \ll 1$, where the subscript g is for grains, etc.), equation (38) reduces to the expression for V_B given just below equation (37); although electrons are also frozen in because $|\tau_e \omega_e| \gg \tau_i \omega_i \gg 1$, their contribution can be neglected in comparison with that of ions.

The magnetic flux Φ of the condensation changes with time according to

$$\frac{1}{\Phi} \frac{d\Phi}{dt} = -\frac{2v_B}{R} = -\frac{1}{\hat{t}_B} \frac{4Z}{R} \left(1 - \frac{3}{f_p} \frac{a_z}{a} \frac{Z}{R}\right), \quad (39)$$

where

$$\hat{t}_B = \frac{A}{A_1} \frac{3}{2\pi a G \rho^2}. \quad (40)$$

Because $f_p \approx 3$ and a_z is nearly equal to a , we can approximate the part containing Z/R in equation (39) as $4(Z/R)(1 - Z/R)$, which is accurate at $Z/R \approx 1$ and whose error decreases as Z/R decreases at somewhat small Z/R . This takes a maximum value of 1 at $Z/R = \frac{1}{2}$. Because the values of ρ and B of the condensation are kept constant during the flux loss as long as Φ is considerably larger than Φ_{cr} , \hat{t}_B is also kept constant. Therefore, \hat{t}_B gives a *minimum* value of the (instantaneous) e -folding time of the magnetic flux, $t_B \equiv -(d \ln \Phi / dt)^{-1}$. For $Z/R \ll 1$, t_B is much larger than \hat{t}_B . For $Z \approx R$, t_B is also much larger than \hat{t}_B , because in such a situation, the pressure force nearly balances the gravitational force not only along the magnetic field lines but also across them, and therefore the magnetic force almost vanishes as in a nearly uniform magnetic field.

To calculate \hat{t}_B , we need the densities of various charged particles. As an example, we show in Figure 6 the abundances of various charged particles as functions of the density n_H . The gas is assumed to have the chemical composition expected in the interstellar clouds (for details see Umebayashi & Nakano 1990). We have assumed that the condensation is shielded from UV radiation and that the gas is ionized by cosmic rays whose intensity has been chosen so as to give the ionization rate of an H_2 molecule, $1 \times 10^{-17} \text{ s}^{-1}$. In addition to various gas-phase reactions, we have considered recombination of ions and electrons at grain surfaces. We have assumed that 20% of carbon and oxygen and 2% of metallic elements are in the gas phase and the rest in grains, and we adopted the power-law size distribution of grains proposed by Mathis, Rumpl, & Nordsieck (1977; hereafter MRN), $dn_g/da_g = C n_H a^{-3.5}$, for grain radius a_g between $a_g^{\min} = 10 \text{ nm}$ and $a_g^{\max} = 250 \text{ nm}$ with $C = 1.5 \times 10^{-25} \text{ cm}^{2.5}$ (MRN; Draine & Lee 1984; Mathis 1986). We have set the gas temperature $T = 10 \text{ K}$. The other details are essentially the same as in Nishi et al. (1991). In Figure 6, g^x , M^+ , and m^+ stand for grains of charge x , metallic ions, and molecular ions other than H_2^+ and H_3^+ , respectively. Although the grains of some charge states other than those shown in this figure have also been taken into account, their abundances are too low to appear in the figure.

Because the grain-surface recombination of ions and electrons is important in determining the densities of various ions, we have investigated several grain models. Figure 7 shows the total ion density n_i for four grain models. Three are on grains without ice mantles with the MRN size dis-

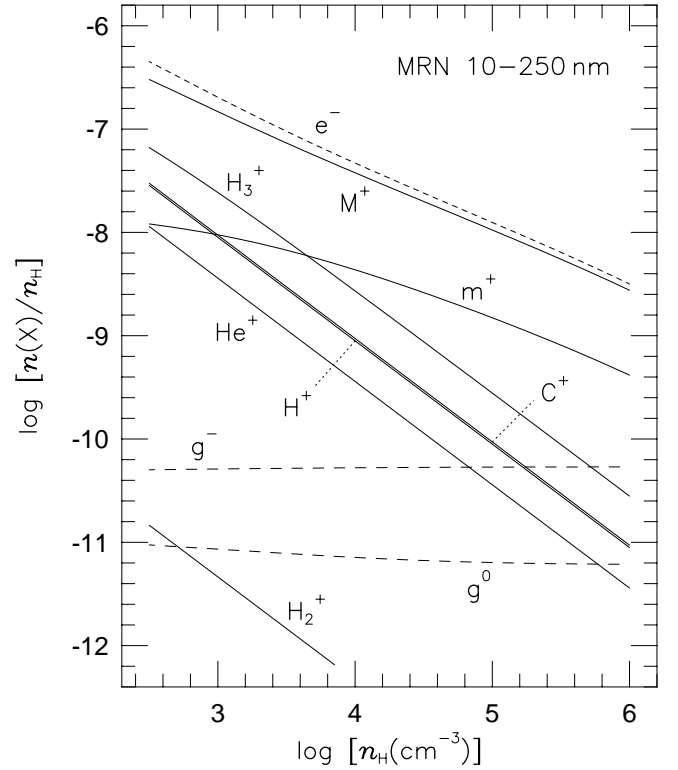


FIG. 6.—Abundances of various charged particles in cloud cores and condensations as functions of n_H . The gas is assumed to have the chemical composition expected in the interstellar clouds (for details, see Umebayashi & Nakano 1990). The cores and condensations are assumed to be shielded from UV radiation but are thin enough to be penetrated by cosmic rays. The cosmic ray intensity is chosen so as to give the ionization rate of an H_2 molecule as $1 \times 10^{-17} \text{ s}^{-1}$. It is assumed that 20% of carbon and oxygen and 2% of metallic elements are in the gas phase and the rest are in grains and that grains have the MRN size distribution for radius a_g between $a_g^{\min} = 10 \text{ nm}$ and $a_g^{\max} = 250 \text{ nm}$. The gas temperature is chosen to be $T = 10 \text{ K}$. Each line is labeled with the corresponding particle name: g^x , M^+ , and m^+ stand for grains of charge x , metallic ions, and molecular ions other than H_2^+ and H_3^+ , respectively.

tribution with $a_g^{\min} = 2, 5, \text{ and } 10 \text{ nm}$ (a_g^{\max} is fixed to 250 nm). Because the $3 \mu\text{m}$ water-ice features are observed in the spectra of stars with $A_V \gtrsim 3.3 \text{ mag}$ (Whittet et al. 1988), we have also investigated ice-mantled grains with the assumption that grains have an MRN distribution with respect to core radii between 10 and 250 nm and have ice mantles of thickness 27 nm. The dotted line shows the ion density for this case but almost overlaps the line for the case of 5 to 250 nm grains without ice mantles. The other details are the same as in Figure 6. For all cases, the ionization fraction is well approximated by $n_i/n_H \propto n_H^{-0.6}$, at least in the density range $10^3 \lesssim n_H \lesssim 10^5 \text{ cm}^{-3}$. The total ion density and the charge state of grains are not very sensitive to the depletion degree of heavy elements from the gas phase, as shown by Umebayashi & Nakano (1990).

If ions are frozen in to the magnetic field and the contribution of charged grains to connecting the magnetic field with neutral gas particles is negligible, \hat{t}_B in equation (40) reduces to

$$\hat{t}_B = \frac{3v_i}{2\pi a G \rho} \frac{\rho_i}{\rho}, \quad (41)$$

which is determined only by the ionization fraction ρ_i/ρ , irrespective of the effective sound velocity C_{eff} , the field strength B , and the density ρ because $v_i \propto \rho$. In general,

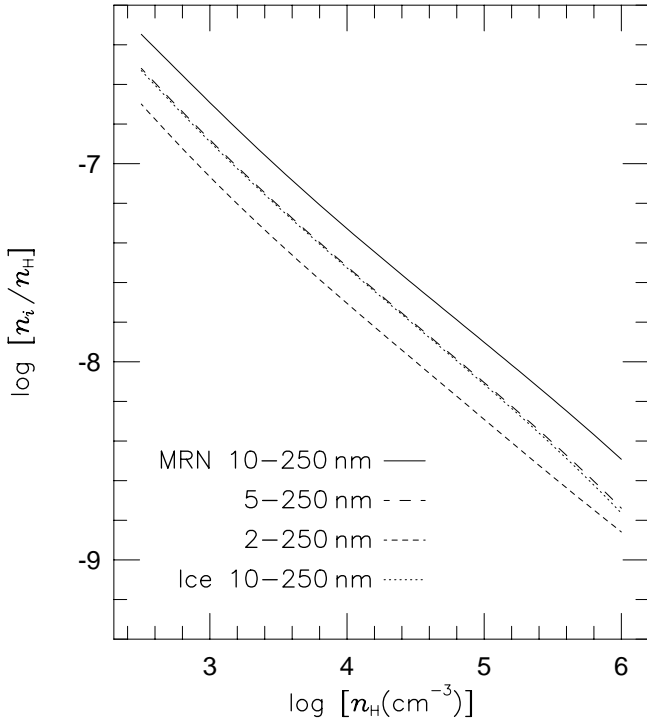


FIG. 7.—Total ion density n_i in cloud cores and condensations as a function of n_H for four cases of the grain model. The cores and condensations are assumed to be shielded from UV radiation and ionized by cosmic rays, whose intensity has been chosen so as to give the ionization rate of an H_2 molecule as $1 \times 10^{-17} \text{ s}^{-1}$. Three cases of grains without ice mantles are shown; the MRN size distribution with the minimum radius $a_g^{\min} = 2, 5$, and 10 nm (the maximum radius a_g^{\max} is fixed to 250 nm). The dotted line shows n_i for the case of ice-mantled grains with an MRN distribution with respect to core radii between 10 and 250 nm with ice mantles of thickness 27 nm , but this line nearly overlaps the line for grains with $a_g^{\min} = 5 \text{ nm}$ without ice mantles.

when some charged particles are not well frozen in, as is usually the case for large grains, \hat{t}_B depends also on ρ and B . In the numerical calculation of \hat{t}_B , we take

$$B \approx B_0 \approx 2\pi C_{\text{eff}} \rho^{1/2} \frac{\Phi_0}{\Phi_{\text{cr0}}} . \quad (42)$$

The last equality has been obtained from equation (13) with $C_{\text{eff}}^2 \rho \approx P_s \approx G\Sigma_0^2$. Figure 8 shows \hat{t}_B as a function of the density n_H for $C_{\text{eff}} = 0.2 \text{ km s}^{-1}$ and $\Phi_0/\Phi_{\text{cr0}} = 0.707$ for the same cases for the grain models as in Figure 7; three cases are for grains without ice mantles and one is for ice-mantled grains. We have used the coefficient of gravity $a = 1.0$ in equation (40). The free-fall time $t_{\text{ff}} = (3\pi/32G\rho)^{1/2}$ is shown by the dot-dashed line for comparison. We have also investigated several cases with C_{eff} between 0.2 and 1.0 km s^{-1} and with Φ_0/Φ_{cr0} between 0.707 and 0.25 and found that \hat{t}_B is not very sensitive to these parameters, at least in these ranges of the parameters and in the density range of Figure 8. Nishi et al. (1991) also showed that \hat{t}_B is not very sensitive to the depletion degree of heavy elements from the gas phase. In the wide range of the grain model, \hat{t}_B takes 10 to 10^2 times t_{ff} in this density range. If the condensation is not well shielded from UV radiation, the ion density is much higher than is shown in Figure 7, and hence \hat{t}_B is much larger than in Figure 8.

Interaction of charged grains with a magnetic field contributes significantly to \hat{t}_B even in the density range of Figure 8. When this interaction is neglected for the case of

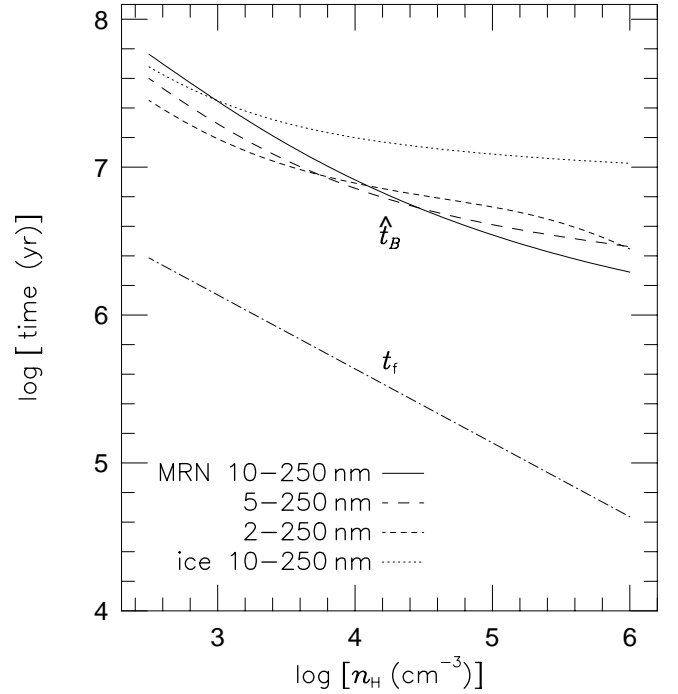


FIG. 8.—Characteristic timescale of magnetic flux loss, \hat{t}_B , in magnetically subcritical condensations embedded in a molecular cloud of magnetic flux $\Phi_0/\Phi_{\text{cr0}} = 0.707$ as a function of n_H . As shown in the text, \hat{t}_B gives the minimum value of the e -folding time of the magnetic flux, $t_B = -(d \ln \Phi / dt)^{-1}$. The condensations are assumed to be shielded from UV radiation and ionized by cosmic rays at a rate of $1 \times 10^{-17} \text{ s}^{-1}$ for H_2 molecules. The effective sound velocity in the condensation is chosen to be $C_{\text{eff}} = 0.2 \text{ km s}^{-1}$. The same grain models as in Fig. 7 are adopted. The free-fall time $t_{\text{ff}} = (3\pi/32G\rho)^{1/2}$ is shown by the dot-dashed line for comparison. It has been found that \hat{t}_B is rather insensitive to Φ_0/Φ_{cr0} and C_{eff} (see text).

the MRN size distribution with $a_g^{\min} = 10 \text{ nm}$, for example, \hat{t}_B becomes smaller than the value shown by the solid line in Figure 8 by a factor of 2.2 at $n_H = 1 \times 10^5 \text{ cm}^{-3}$, though it is smaller by less than 30% at $n_H < 1 \times 10^4 \text{ cm}^{-3}$. When a condensation is not well shielded from UV radiation and the ion density is much higher than those in Figure 7, interaction of charged grains with the magnetic field contributes little to \hat{t}_B , and equation (41) holds in good approximation.

For a given mass of the condensation, we have $\Phi \propto (Z/R)^{-2/3}$ as long as ρ and B are kept constant. Because \hat{t}_B is also kept constant under these circumstances, we can easily integrate equation (39). The time required to decrease Φ by some specified factor depends on the initial (or final) value of Z/R and takes a minimum value at a certain initial (or final) value of Z/R . For example, to decrease Φ by factors of 2 and e takes at least $0.76\hat{t}_B$ and $1.21\hat{t}_B$, respectively. Thus, \hat{t}_B gives a good estimate of the minimum value of the time required for a condensation to lose a significant fraction of its magnetic flux. Because $\Sigma = M/\pi R^2 = MB/\Phi$, \hat{t}_B also gives the minimum value for the timescale of column density increase.

Because the field strength B given by equation (42) is independent of the flux Φ/Φ_{cr} of the condensation, \hat{t}_B does not depend on Φ/Φ_{cr} as long as Φ is considerably larger than Φ_{cr} . Moreover, the value of \hat{t}_B given by equation (40) is almost the same as the characteristic timescale of magnetic flux loss from the central part of a magnetically critical cloud obtained by setting $B = B_{\text{cr}}$ in equation (22) of Nishi et al. (1991), and the critical field B_{cr} given by equation (19)

of Nishi et al. is nearly equal to B in equation (42) as long as $\Phi_0/\Phi_{\text{cr}0} \sim 1$. Therefore, the flux loss time is nearly independent of Φ/Φ_{cr} at $\Phi/\Phi_{\text{cr}} \gtrsim 1$. On the other hand, the characteristic flux loss time from the central part of a magnetically supercritical cloud ($\Phi/\Phi_{\text{cr}} < 1$) is obtained by multiplying the right-hand side of equation (40) by $(\Phi_{\text{cr}}/\Phi)^2$ or $(B_{\text{cr}}/B)^2$, as shown in equation (22) of Nishi et al. (see also Nakano & Umebayashi 1986).

5.2. Comparison with Other Works on Magnetically Subcritical Clouds

The evolution of magnetically subcritical condensations described above is quite different from some of the recent results on the contraction of subcritical clouds via ambipolar diffusion. In contrast to early works on quasi-static contraction that dealt with clouds that initially are barely subcritical (Nakano 1979, 1982, 1983), most recent works assume highly subcritical initial states (Fiedler & Mouschovias 1993; Ciolek & Mouschovias 1994; Basu & Mouschovias 1994; Safier et al. 1997). For example, Ciolek & Mouschovias (1994) made numerical simulations of model clouds that initially have magnetic flux $\Phi = 3.9\Phi_{\text{cr}}$ and are under external pressure (P_s in our notation) equal to nearly 1/10 times the “gravitational pressure” $\pi G \Sigma^2/2$ at the initial state, Σ being the column density of the cloud along the mean direction of magnetic field, and found that the clouds contract quasi-statically, enhancing the density in their central parts. Highly magnetically subcritical clouds under such low external pressure expand almost freely unless they are immersed in a sufficiently strong external magnetic field. In reality, the figures of Ciolek & Mouschovias show that the initial magnetic field is almost uniform on the midplane of the cloud, and therefore it must initially be almost uniform everywhere, as inferred from their boundary condition that the magnetic field far away from the cloud should be uniform with some specified strength and perpendicular to the midplane. In numerical simulations with such boundary conditions, the magnetic field lines are pinned at the outer boundaries of the computation region, and hence the cloud can be in an equilibrium state no matter how large its magnetic flux is.

However, molecular clouds are magnetically supercritical, as shown by McKee et al. (1993) and in § 2.1. The clouds adopted by Ciolek & Mouschovias (1994) initially have nearly uniform magnetic fields of about $35 \mu\text{G}$. Because this is much stronger than the field of several μG expected in the diffuse interstellar medium (Davies et al. 1963), such clouds cannot be confined by the interstellar magnetic field. The initial field has a magnetic pressure of about $3.5 \times 10^5 \text{ cm}^{-3} \text{ K}$, which is much higher than the pressure of the diffuse interstellar medium (see § 2). Even if such a high pressure were provided by the ambient medium, it would contradict the low external pressure they assumed; the discrepancy is by a factor of 150.

Magnetically subcritical condensations may be able to exist in molecular clouds, as discussed in § 5.1. For $\Phi = 3.9\Phi_{\text{cr}}$, equation (14) gives $\Sigma/\Sigma_0 \approx 0.29\Phi_0/\Phi_{\text{cr}0}$ if the term with Z/R is neglected; Σ/Σ_0 is even smaller for a nonzero Z/R . Because the cloud is magnetically supercritical ($\Phi_0/\Phi_{\text{cr}0} < 1$), the column density Σ of such a condensation is much lower than that of the cloud, Σ_0 . Except near its surfaces, the cloud has an internal pressure $P_s \approx G \Sigma_0^2$, which is more than an order of magnitude higher than the gravitational pressure of this condensation, $\pi G \Sigma^2/2$, and

thus more than 2 orders of magnitude higher than the external pressure Ciolek & Mouschovias (1994) assumed. Magnetically subcritical condensations are confined by pressure unless they are located very close to the cloud surface.

A magnetically subcritical condensation with low surface pressure can exist only near the cloud surface. The surface pressure can be smaller than the condensation’s own gravitational pressure only when it is located at a depth $\Delta \Sigma_0 < \Sigma^2/4\Sigma_0$ from the cloud surface, or $\Delta \Sigma_0/\Sigma_0 < 0.02(\Phi_0/\Phi_{\text{cr}0})^2$ for $\Sigma/\Sigma_0 \approx 0.29\Phi_0/\Phi_{\text{cr}0}$, very close to the cloud surface. Such condensations must be exposed to interstellar UV radiation and must be extremely slow in contraction as discussed in § 2.3.

Star formation in such highly magnetically subcritical condensations with low surface pressure faces another difficulty. Ciolek & Mouschovias (1994; see also Ciolek 1996) found that a significant amount of grains are lost from the central part of a cloud in the course of contraction. The final abundance of grains in the central part is about 1/3.9 times the initial abundance; the reduction factor of the grain abundance is nearly equal to the reduction factor of the magnetic flux. If such extensive loss of grains actually occurs in the course of star formation, heavy elements in those stars must be much less abundant than in the molecular clouds because most of the heavy elements are estimated to be in grains, even in diffuse clouds (Morton 1974). There are no observations supporting such a large difference in the abundance of heavy elements between molecular clouds and young stars. On the other hand, Nakano (1984) and Nakano, Nishi, & Umebayashi (1996) showed that very few grains are lost in the course of star formation in magnetically supercritical cloud cores. This difference stems from two facts: the fact that, in highly magnetically subcritical clouds with low surface pressure, the magnetic field is much stronger than is given by equation (42) at a given density, and hence even large grains may be frozen in to magnetic field; and the fact that prior to the onset of dynamical contraction, highly magnetically subcritical clouds must lose most of their initial magnetic flux at low densities where $|\tau_g \omega_g|$ is large, while magnetically supercritical clouds lose most of their magnetic flux at very high densities where even the smallest grains are just barely frozen in (Nakano 1984; Nakano et al. 1996). This could be more counterevidence, in addition to that shown in § 2, for the assumption that low-mass stars form mainly in magnetically subcritical cloud cores.

6. DISCUSSION

6.1. Velocity Dispersions and Formation Processes of Cloud Cores

We found in § 2 that the observed cloud cores are magnetically supercritical. If such a core forms from magnetically subcritical condensations via ambipolar diffusion, its formation time must be nearly equal to the magnetic flux loss time t_B , which is more than 10 times larger than the free-fall time t_{ff} . As long as there are no sources to drive turbulence and hydromagnetic waves, turbulence dissipates in several times t_{ff} and hydromagnetic waves decay in $10^{-2}t_B$, as shown in the Appendix. Because most cloud cores are not translucent, disturbances from the outside are not efficient in exciting the waves. Therefore, if the cores form from magnetically subcritical condensations via ambipolar diffusion, the velocity dispersions of the cores not

accompanied by YSOs must be very small, contradicting the observational results.

Because the turbulence in the cores dissipates in several times the free-fall time and because hydromagnetic waves dissipate in a free-fall time and are only slightly excited by disturbances from the outside, the turbulence observed in the cores without YSOs must be the turbulence generated when the cores were formed and must be dissipating. Therefore, I speculate that the cores form in the following way. Condensations that have begun dynamical contraction soon settle down into virial equilibrium by randomizing the contraction motion; randomization of the motion most probably occurs in considerably asymmetric condensations. One can imagine some processes by which the condensations begin dynamical contraction. For example, condensations will form by compression of the cloud matter by turbulence (Norman & Silk 1980) and grow by coalescence and finally begin dynamical contraction when they have grown beyond the critical state for dynamical contraction (Field & Saslaw 1965). The condensations growing in this way must be far from symmetric. The condensations formed by gravitational instability of the cloud also contract dynamically.

The turbulence of the core formed in this way is transient. It decays in several times the free-fall time of the core, and stars form unless the core mass is so small that P_{cr} is higher than the pressure of the ambient medium even after the turbulence has dissipated. The mass outflows from the YSOs in the core can enhance the velocity dispersion of the core but finally disintegrate the core by blowing off the core matter (Nakano, Hasegawa, & Norman 1995). Thus, the cores formed in this way can maintain the velocity dispersions nearly equal to their virial velocities for a significant fraction of their lifetimes, which is consistent with the observations.

6.2. Initial State of Dynamical Contraction and Accretion Rate

We have found that the dynamical contraction of a cloud core sets in when the critical surface pressure P_{cr} given by equations (19) and (27) falls to the pressure of the surrounding medium P_s . The Bonnor-Ebert isothermal cloud also behaves in the same way. At the critical state with surface pressure $P_s = P_{\text{cr}}^{\text{BE}}$, the Bonnor-Ebert cloud has a central part of nearly uniform density (density higher than $\rho_c/2$) with radius $2.3C_s(4\pi G\rho_c)^{-1/2}$, where ρ_c is the density at the center. Outside this part, the density is approximately proportional to r^{-2} and the surface is reached (the pressure falls to P_s) at $6.45C_s(4\pi G\rho_c)^{-1/2}$. The mass of this central part is about one-sixth of the total mass of the cloud. Although we cannot determine the detailed structure of the cloud core on the basis of the virial theorem, the magnetic cloud core at the critical state must also have a nearly uniform central part. Recent submillimeter- and millimeter-wave observations of some cloud cores suggest that the density profile flattens near their centers (Ward-Thompson et al. 1994; André et al. 1996), supporting the above discussion.

A high probability of multiplicity has been observed among pre-main-sequence stars (Simon et al. 1992). Existence of fairly large uniform central parts in the cores at the onset of dynamical contraction must be favorable for the formation of multiple stars as discussed by Whitworth et al. (1996).

Because the cloud core has a flattened density profile near its center at the onset of dynamical contraction, the accretion rate onto the central protostellar object cannot be kept constant. It must be significantly larger than the standard rate $0.975C_{\text{eff}}^3/G$ (Shu 1977) in the early stage and must decrease with time, as shown by the numerical simulations of Foster & Chevalier (1993) and Tomisaka (1996).

6.3. Timescale of Star Formation

Fuller & Myers (1987) discussed the amount of time for which cloud cores exist before they form stars. From the statistics of the cores with and without *IRAS* sources in several nearby molecular clouds, they concluded that a core stays in the equilibrium state only for about its free-fall time. From the statistical analysis of cloud cores and young stellar objects in the Taurus molecular cloud, T. Onishi, A. Mizuno, A. Kawamura, H. Ogawa, & Y. Fukui (1996, private communication) found that the cloud cores stay in the phase not associated with *IRAS* sources for $2\text{--}4 \times 10^5$ yr, which is several times the free-fall time for the mean density of the cores, $n_{\text{H}} \approx 2 \times 10^5 \text{ cm}^{-3}$.

As shown in § 4, magnetically supercritical cloud cores begin to collapse when a significant fraction of their initial turbulence has dissipated, except in the cases of cores of very small mass with nearly critical magnetic flux with $1 - (\Phi/\Phi_{\text{cr}})^2 \ll 1$. This dissipation occurs in several times the free-fall time. To form stars, the cloud cores of small mass with $a_{\text{eff}} = a[1 - (\Phi/\Phi_{\text{cr}})^2] \ll 1$, if they exist, must enhance a_{eff} by magnetic flux loss, as well as by dissipation of turbulence. Only a slight loss of magnetic flux is enough to cause this effect, which takes only a small fraction of the e -folding time of the magnetic flux t_B . Therefore, the star formation time in such cores must not be much different from the dissipation time of their turbulence. Thus, our result in § 4 agrees well with the conclusion of Onishi et al. (1996, private communication) and does not seem to seriously contradict the conclusion of Fuller & Myers (1987).

6.4. Lifetime of Molecular Clouds

Although the lifetime of each cloud core is nearly equal to the dissipation time of turbulence, which is several times the free-fall time of the cores, the lifetime of the molecular cloud that contains many cloud cores must be much longer. Nakano et al. (1995) showed that the star formation efficiency in each core is very low; most of the core matter is blown off by mass outflows from the forming stars in the core and by the expansion of compact H II regions developed by them. Because the final velocity of the matter ejected by the mass outflow is not so large (Nakano et al. 1995), the matter will remain in the cloud and excite turbulence in the cloud. Because molecular clouds seem to be ionized mainly by UV radiation and have much higher ionization fractions than the cloud cores (Myers & Khersonsky 1995), hydromagnetic waves may dissipate rather slowly. Cloud cores must be formed repeatedly in such a turbulent cloud (Norman & Silk 1980), and the lifetime of the cloud as a whole must be much longer than that of an individual cloud core.

7. SUMMARY AND CONCLUSION

We have reexamined the widely accepted assumption that low-mass stars form mainly in magnetically subcritical cloud cores while high-mass stars form in magnetically supercritical ones, and we have investigated the processes

that put the cloud cores in magnetohydrostatic equilibrium to dynamical contraction. The main results are as follows.

1. As well as molecular clouds, cloud cores embedded in clouds are shown to be magnetically supercritical for several reasons. First, although cloud cores are generally observed as portions of a molecular cloud having column densities somewhat higher than the mean column density of the cloud, magnetically subcritical condensations are unlikely to have column densities higher than their surroundings. Second, if cloud cores are magnetically subcritical, it is difficult to maintain for a significant fraction of their lifetimes the nonthermal velocity dispersions widely observed in the cores.

2. For a magnetically supercritical cloud core, there is a critical value P_{cr} for the surface pressure P_s ; when $P_s > P_{cr}$, the core cannot be in magnetohydrostatic equilibrium and collapses. The pressure P_{cr} is sensitive to the core mass M , the effective sound velocity in the core C_{eff} , and the effective coefficient for gravity diluted by magnetic force, a_{eff} , as shown in equations (19) and (27).

3. A core in magnetohydrostatic equilibrium begins to contract dynamically when P_{cr} has decreased to P_s by some mechanism. The most important mechanism in reducing P_{cr} is the dissipation of turbulence in the core. Because the fractional contribution of turbulence to C_{eff} tends to be higher in the observed cloud cores with higher mass, dynamical contraction tends to set in more easily in cores with higher mass. The timescale of star formation in such a core is therefore the dissipation time of its turbulence, which is several times the free-fall time of the core.

4. For cores with small a_{eff} or with magnetic flux Φ very close to the critical magnetic flux Φ_{cr} , P_{cr} will not decrease below P_s even when the turbulence has dissipated significantly. This will happen only in very low mass cores

because P_{cr} is sensitive to the core mass. Such a core begins dynamical contraction after a_{eff} has increased somewhat because of magnetic flux loss by ambipolar diffusion in the central part of the core. Only a slight loss of magnetic flux is needed for this to occur because P_{cr} is very sensitive to Φ at $\Phi \approx \Phi_{cr}$, and hence contraction takes a time much shorter than the e -folding time of magnetic flux. Therefore, the time required for star formation is not much different from the dissipation time of the turbulence. However, the probability that a core initially has Φ very close to Φ_{cr} may be very low.

5. Significantly subcritical condensations in a molecular cloud, if they exist, have column densities considerably lower than the mean column density of the cloud. This means that the condensations are confined by pressure and have nearly uniform densities as long as C_{eff} is constant in each condensation unless they are located very close to the cloud surface. Growth of such condensations to magnetically supercritical cores via ambipolar diffusion takes at least 10 to 10^2 times the free-fall time if they are well shielded from UV radiation, and it takes much longer time if they are not well shielded.

6. It is highly implausible that cloud cores form from magnetically subcritical condensations via ambipolar diffusion because it is difficult for the condensations to keep nonthermal velocity dispersions, which are widely observed in cloud cores, until they grow into cores.

I would like to thank K. Tatematsu for valuable comments and discussions. I am also grateful to T. Hasegawa, M. Hayashi, S. Inutsuka, S. M. Miyama, M. Momose, T. Onishi, K. Sunada, and M. Tamura for valuable discussions.

APPENDIX

DISSIPATION AND EXCITATION OF HYDROMAGNETIC WAVES IN MOLECULAR CLOUDS AND CLOUD CORES

Various molecular lines observed in molecular clouds and cloud cores usually have widths much larger than their thermal widths, and the widths are interpreted as caused by turbulence and/or hydromagnetic wave motion. If there are some driving sources in clouds or cloud cores, not only turbulence but also hydromagnetic waves can be maintained (Gammie & Ostriker 1996). We investigate here the dissipation and the possibility of excitation of waves in molecular clouds and in condensations embedded in molecular clouds, which do not have internal driving sources.

Kulsrud & Pearce (1969) made normal-mode analysis of Alfvén waves in slightly ionized gas. For waves satisfying $v_i \gg \omega_k \equiv kV_{Ai}$, where v_i is the collision frequency of an ion with neutral molecules and is equal to $\rho \langle \sigma v \rangle / m_i$ or to the inverse of the viscous damping time of ions τ_i in § 5.1, k is the wave number, and $V_{Ai} = B(4\pi\rho_i)^{-1/2}$ is the Alfvén velocity of the ion waves, ρ_i being the density of the ions, they found the dispersion relation

$$\omega = \pm \left(\omega_k^2 \frac{\rho_i}{\rho} - \frac{\omega_k^4}{4v_i^2} \right)^{1/2} - i \frac{\omega_k^2}{2v_i}. \quad (43)$$

In terms of the wavelength $\lambda = 2\pi/k$ and the thickness $2Z$ along magnetic field lines of the cloud or of the condensation embedded in a cloud, the condition for this relation to hold, $v_i \gg \omega_k$, can be rewritten as

$$\frac{\lambda}{2Z} \gg 1.3 \times 10^{-3} \frac{\Phi}{\Phi_{cr}} \left(\frac{n_H}{1 \times 10^3 \text{ cm}^{-3}} \right)^{-1/2} \left(\frac{n_i/n_H}{1 \times 10^{-7}} \right)^{-1/2} \left(\frac{m_i}{28m_H} \right)^{1/2} \left(\frac{f_\phi}{2\pi} \right). \quad (44)$$

In deriving this equation, we have used the relation

$$B = 2Z\rho f_\phi G^{1/2} \frac{\Phi}{\Phi_{cr}}, \quad (45)$$

which is obtained from equation (12), and have set $\langle \sigma v \rangle = 1.5 \times 10^{-9} \text{ cm}^3 \text{ s}^{-1}$. The ionization fraction n_i/n_H is normalized to the value in the clouds shielded from UV radiation and ionized mainly by cosmic rays (see Fig. 7). Because n_i/n_H is nearly proportional to $n_H^{-0.6}$ in such clouds, the right-hand side of equation (44) depends only weakly on the density ($\propto n_H^{-0.2}$). Although the wavelength is restricted to $\lambda \lesssim 2Z$, equation (43) is applicable to a wide range of wavelengths in molecular clouds and condensations.

The wave can propagate only when it has a nonvanishing real part ω , or when

$$\Psi \equiv \frac{k V_A}{2v_i} \frac{\rho}{\rho_i} = \frac{k V_A}{2v_n} \quad (46)$$

is smaller than 1, where $V_A = B(4\pi\rho)^{-1/2}$ is the Alfvén velocity and $v_n = v_i(\rho_i/\rho)$ is the collision frequency of a neutral molecule with ions. The condition for the wave propagation, $\Psi < 1$, can be rewritten as

$$\frac{\lambda}{2Z} > 0.46 \frac{\Phi}{\Phi_{\text{cr}}} \left(\frac{n_H}{1 \times 10^3 \text{ cm}^{-3}} \right)^{-1/2} \left(\frac{n_i/n_H}{1 \times 10^{-7}} \right)^{-1} \left(\frac{f_\phi}{2\pi} \right). \quad (47)$$

In clouds and condensations well shielded from UV radiation, the right-hand side of equation (47) depends only slightly on the density ($\propto n_H^{0.1}$), and only some restricted waves can propagate unless $\Phi \ll \Phi_{\text{cr}}$. In clouds and condensations not well shielded from UV radiation and having higher ionization fractions, waves with a wider range of wavelengths can propagate.

From equation (43), we find that the waves with $\Psi < 1$ decay in a timescale

$$t_{\text{dis}} = \frac{2v_i}{\omega_k^2} = \frac{1}{2v_n\Psi^2} = \frac{v_i}{2\pi^3 G\rho} \frac{\rho_i}{\rho} \left(\frac{\Phi_{\text{cr}}}{\Phi} \right)^2 \left(\frac{\lambda}{2Z} \right)^2 \left(\frac{f_\phi}{2\pi} \right)^{-2}. \quad (48)$$

It is to be noted that shorter waves dissipate more quickly. Because t_{dis} has the same dependence on v_i and ρ_i/ρ as \hat{t}_B , given by equation (41), equation (48) can be rewritten as

$$t_{\text{dis}} = \frac{a}{3\pi^2} \hat{t}_B \left(\frac{\Phi_{\text{cr}}}{\Phi} \right)^2 \left(\frac{\lambda}{2Z} \right)^2 \left(\frac{f_\phi}{2\pi} \right)^{-2}. \quad (49)$$

As shown in § 5.1, \hat{t}_B gives a minimum value of the timescale of magnetic flux loss, t_B , for $\Phi/\Phi_{\text{cr}} > 1$, and $(\Phi_{\text{cr}}/\Phi)^2 \hat{t}_B$ gives the flux loss time t_B from the central part of the core for $\Phi/\Phi_{\text{cr}} < 1$. If the velocity dispersion is caused by the wave motion, the waves of λ somewhat smaller than $2Z$ must have large amplitudes. For such waves, t_{dis} is smaller than $10^{-2} t_B$.

In units of the free-fall time $t_{\text{ff}} = (3\pi/32G\rho)^{1/2}$, t_{dis} in equations (48) and (49) is rewritten as

$$\frac{t_{\text{dis}}}{t_{\text{ff}}} = 0.36 \left(\frac{\Phi_{\text{cr}}}{\Phi} \right)^2 \left(\frac{\lambda}{2Z} \right)^2 \left(\frac{n_H}{1 \times 10^3 \text{ cm}^{-3}} \right)^{1/2} \left(\frac{n_i/n_H}{1 \times 10^{-7}} \right) \left(\frac{f_\phi}{2\pi} \right)^{-2} \quad (50)$$

$$= 0.34 \left(\frac{\Phi_{\text{cr}}}{\Phi} \right)^2 \left(\frac{\lambda}{2Z} \right)^2 \left(\frac{\hat{t}_B/t_{\text{ff}}}{10} \right) \left(\frac{f_\phi}{2\pi} \right)^{-2}. \quad (51)$$

In deriving equation (51), we have used the coefficient of the gravity $a = 1.0$ as in Figure 8. In clouds and condensations that are well shielded from UV radiation, the right-hand side of equation (50) depends only slightly on the density ($\propto n_H^{-0.1}$), and therefore the waves with λ somewhat smaller than $2Z$ decay in a timescale significantly shorter than t_{ff} if $\Phi > \Phi_{\text{cr}}$, and in a timescale shorter than t_{ff} unless $(\Phi/\Phi_{\text{cr}})^2 \ll 1$. If $(\Phi/\Phi_{\text{cr}})^2 \ll 1$, large-amplitude wave motions must be supersonic and super-Alfvénic, and shock dissipation must occur on a timescale much shorter than t_{dis} given above.

For waves of shorter wavelengths satisfying $\Psi > 1$, ω is purely imaginary, and there are two modes with different decay timescales; one has a decay time smaller than that given by equation (48), and another has one larger. At $\Psi \gg 1$, the decay time of the latter mode is approximately given by

$$\tilde{t}_{\text{dis}} \equiv v_n^{-1}, \quad (52)$$

regardless of the magnetic field strength. At Ψ not much smaller than one, the decay time is smaller than \tilde{t}_{dis} and $t_{\text{dis}} = \tilde{t}_{\text{dis}}/2$ at $\Psi = 1$, as seen from equation (48). Thus \tilde{t}_{dis} gives an upper bound to the dissipation time of the waves with $\Psi \geq 1$ and is represented numerically as

$$\frac{\tilde{t}_{\text{dis}}}{t_{\text{ff}}} = 0.15 \left(\frac{n_H}{1 \times 10^3 \text{ cm}^{-3}} \right)^{-1/2} \left(\frac{n_i/n_H}{1 \times 10^{-7}} \right)^{-1}. \quad (53)$$

In clouds and condensations well shielded from UV radiation, \tilde{t}_{dis} is much smaller than t_{ff} at least at $n_H \lesssim 10^6 \text{ cm}^{-3}$. In clouds and condensations not well shielded, \tilde{t}_{dis} is even smaller. Thus, all the waves with $\Psi > 1$ decay on a timescale much smaller than t_{ff} .

The phase velocity of the waves with $\Psi < 1$ is given by $V_{\text{ph}} = \omega_r/k = V_A(1 - \Psi^2)^{1/2}$, where ω_r is the real part of ω . The crossing time of the waves across the cloud or condensation is then given by

$$t_{\text{cross}} \equiv \frac{2Z}{V_{\text{ph}}} = (\pi G\rho)^{-1/2} \left(\frac{\Phi_{\text{cr}}}{\Phi} \right) (1 - \Psi^2)^{-1/2} \left(\frac{f_\phi}{2\pi} \right)^{-1}. \quad (54)$$

The wavelength dependence is through Ψ . Taking the ratio of equations (48) and (54) gives

$$\frac{t_{\text{dis}}}{t_{\text{cross}}} = \frac{1}{2\pi} \frac{\lambda}{2Z} \frac{(1 - \Psi^2)^{1/2}}{\Psi}, \quad (55)$$

where Ψ in equation (46) can be rewritten as

$$\Psi = \frac{\pi}{v_i} \frac{\rho}{\rho_i} (\pi G \rho)^{1/2} \left(\frac{\Phi}{\Phi_{\text{cr}}} \right) \left(\frac{2Z}{\lambda} \right) \left(\frac{f_\phi}{2\pi} \right) \quad (56)$$

$$= 0.46 \left(\frac{\Phi}{\Phi_{\text{cr}}} \right) \left(\frac{2Z}{\lambda} \right) \left(\frac{n_{\text{H}}}{1 \times 10^3 \text{ cm}^{-3}} \right)^{-1/2} \left(\frac{n_i/n_{\text{H}}}{1 \times 10^{-7}} \right)^{-1} \left(\frac{f_\phi}{2\pi} \right) \quad (57)$$

$$= 0.49 \left(\frac{\Phi}{\Phi_{\text{cr}}} \right) \left(\frac{2Z}{\lambda} \right) \left(\frac{\hat{t}_B/t_{\text{ff}}}{10} \right)^{-1} \left(\frac{f_\phi}{2\pi} \right). \quad (58)$$

Equation (58) has been derived by using equation (41). For the waves with λ somewhat smaller than $2Z$, t_{dis} is considerably smaller than t_{cross} for clouds and condensations well shielded from UV radiation unless $\Phi/\Phi_{\text{cr}} \ll 1$.

Although Kulsrud & Pearce (1969) did not take into account the interaction of charged grains with a magnetic field, it must have some effect on the propagation and dissipation of the waves. Because \hat{t}_B without charged grains, given by equation (41), has the same dependence on v_i and ρ_i/ρ as do t_{dis} and Ψ^{-1} , the effect of charged grains must be taken approximately into account by using \hat{t}_B with the effect of charged grains, or \hat{t}_B shown in Figure 8 when the cloud or condensation is well shielded from UV radiation, in equations (49), (51), and (58). If the interaction of grains with magnetic field is neglected, \hat{t}_B becomes smaller than the values in Figure 8 by less than 30% at $n_{\text{H}} \leq 1 \times 10^4 \text{ cm}^{-3}$, and by a factor of 2.2 at $n_{\text{H}} = 1 \times 10^5 \text{ cm}^{-3}$ for the case of the MRN size distribution with $a_g^{\text{min}} = 10 \text{ nm}$. Even with this modification, the above conclusions need not be changed; in clouds and condensations that are well shielded from UV radiation and are not highly magnetically supercritical, t_{dis} is smaller than both t_{ff} and t_{cross} . In clouds and condensations not well shielded from UV radiation where the ion density is much higher than those in Figure 7, the contribution of charged grains to \hat{t}_B is small, and equations (50) and (57) hold in good approximation.

To excite the waves by perturbations from the outside takes at least the crossing time t_{cross} of the waves given by equation (54). In clouds and condensations that are well shielded from UV radiation and are not highly magnetically supercritical, the hydromagnetic waves cannot be maintained because t_{dis} is smaller than both t_{ff} and t_{cross} .

If a cloud or condensation is highly magnetically supercritical, the gas motion causing the observed line widths must be supersonic and super-Alfvénic. Because shock dissipation of such motion must occur on a timescale much shorter than t_{dis} given by equations (48), (50), and (51), it must also be difficult to maintain waves in such clouds and condensations.

If a condensation is not well shielded from UV radiation and has a much higher ion density than those shown in Figure 7, t_{dis} may be much larger than t_{ff} and larger than t_{cross} , and therefore hydromagnetic waves may be maintained. On the other hand, \hat{t}_B must also be very large. From equations (55), (57), and (58), $t_{\text{dis}} > t_{\text{cross}}$ requires that

$$\frac{n_i}{n_{\text{H}}} > 3 \times 10^{-7} \left(\frac{n_{\text{H}}}{1 \times 10^3 \text{ cm}^{-3}} \right)^{-1/2} \left(\frac{\Phi}{\Phi_{\text{cr}}} \right) \left(\frac{2Z}{\lambda} \right)^2 \left(\frac{f_\phi}{2\pi} \right), \quad (59)$$

or

$$\frac{\hat{t}_B}{t_{\text{ff}}} > 30 \left(\frac{\Phi}{\Phi_{\text{cr}}} \right) \left(\frac{2Z}{\lambda} \right)^2 \left(\frac{f_\phi}{2\pi} \right). \quad (60)$$

Therefore, to keep the waves with λ somewhat smaller than $2Z$ at large amplitudes in magnetically subcritical condensations, the ionization fraction must be more than 2 orders of magnitude higher than in condensations shielded from UV radiation. In addition, equation (60) means that it takes a very long time, i.e., significantly longer than 10^8 yr in condensations of $n_{\text{H}} \lesssim 10^4 \text{ cm}^{-3}$, to form cloud cores from magnetically subcritical condensations via ambipolar diffusion while keeping the waves at large amplitudes.

REFERENCES

- André, P., Ward-Thompson, D., & Motte, F. 1996, *A&A*, 314, 625
Arons, J., & Max, C. E. 1975, *ApJ*, 196, L77
Bally, J., Langer, W. D., Stark, A. A., & Wilson, R. W. 1987, *ApJ*, 312, L45
Basu, S., & Mouschovias, T. Ch. 1994, *ApJ*, 432, 720
Bertoldi, F., & McKee, C. F. 1992, *ApJ*, 395, 140
Binney, J., & Tremaine, S. 1987, *Galactic Dynamics* (Princeton: Princeton Univ. Press)
Bohlin, R. C., Savage, B. D., & Drake, J. F. 1978, *ApJ*, 224, 132
Bonnor, W. B. 1956, *MNRAS*, 116, 351
Chandrasekhar, S., & Fermi, E. 1953, *ApJ*, 118, 116
Ciolek, G. E. 1996, in *The Role of Dust in the Formation of Stars*, ed. H. U. Käufel & R. Siebenmorgen (Berlin: Springer), 367
Ciolek, G. E., & Mouschovias, T. Ch. 1994, *ApJ*, 425, 142
Cohen, M., & Kuhl, L. V. 1979, *ApJS*, 41, 743
Cox, D. P. 1988, in *Supernova Remnants and the Interstellar Medium*, ed. R. S. Roger & T. L. Landecker (Cambridge: Cambridge Univ. Press), 73
Crutcher, R. M., Mouschovias, T. Ch., Troland, T. H., & Ciolek, G. E. 1994, *ApJ*, 427, 839
Crutcher, R. M., Troland, T. H., Goodman, A. A., Heiles, C., Kazès, I., & Myers, P. C. 1993, *ApJ*, 407, 175
Crutcher, R. M., Troland, T. H., Lazareff, B., & Kazès, I. 1996, *ApJ*, 456, 217
Dame, T. M., Elmegreen, B. G., Cohen, R. S., & Thaddeus, P. 1986, *ApJ*, 305, 892
Davies, R. D., Shuter, W. L. H., Slater, C. H., & Wild, P. A. T. 1963, *MNRAS*, 126, 353
Draine, B. T., & Lee, H. M. 1984, *ApJ*, 285, 89
Ebert, R. 1955, *Z. Astrophys.*, 37, 222
Elmegreen, B. G. 1985, *ApJ*, 299, 196
———. 1989, *ApJ*, 338, 178
Fiedler, R. A., & Mouschovias, T. Ch. 1993, *ApJ*, 415, 680
Field, G. B., & Saslaw, W. C. 1965, *ApJ*, 142, 568

- Foster, P. N., & Chevalier, R. A. 1993, *ApJ*, 416, 303
- Fuller, G. A., & Myers, P. C. 1987, in *Physical Processes in Interstellar Clouds*, ed. G. E. Morfill & M. Scholer (Dordrecht: Reidel), 137
- Gammie, C. F., & Ostriker, E. C. 1996, *ApJ*, 466, 814
- Goldsmith, P. F., & Arquilla, R. 1985, in *Protostars and Planets II*, ed. D. C. Black & M. S. Matthews (Tucson: Univ. Arizona Press), 137
- Goodman, A. A., Benson, P. J., Fuller, G. A., & Myers, P. C. 1993, *ApJ*, 406, 528
- Heiles, C., Goodman, A. A., McKee, C. F., & Zweibel, E. G. 1993, in *Protostars and Planets III*, ed. E. H. Levy & J. I. Lunine (Tucson: Univ. Arizona Press), 279
- Herbig, G. H. 1970, in *Proc. 14th Liege Symp.*, 59, 13
- Kulsrud, R., & Pearce, W. P. 1969, *ApJ*, 156, 445
- Larson, R. B. 1981, *MNRAS*, 194, 809
- Lizano, S., & Shu, F. H. 1989, *ApJ*, 342, 834
- Mathis, J. S. 1986, *ApJ*, 308, 281
- Mathis, J. S., Rumpl, W., & Nordsieck, K. H. 1977, *ApJ*, 217, 425 (MRN)
- McKee, C. F. 1989, *ApJ*, 345, 782
- McKee, C. F., & Zweibel, E. G. 1992, *ApJ*, 399, 551
- McKee, C. F., Zweibel, E. G., Goodman, A. A., & Heiles, C. 1993, in *Protostars and Planets III*, ed. E. H. Levy & J. I. Lunine (Tucson: Univ. Arizona Press), 327
- Mestel, L. 1965, *QJRAS*, 6, 265
- Mestel, L., & Spitzer, L., Jr. 1956, *MNRAS*, 116, 503
- Mezger, P. G., & Smith, L. F. 1977, in *IAU Symp. 75, Star Formation*, ed. T. de Jong & A. Maeder (Dordrecht: Reidel), 133
- Mizuno, A., Onishi, T., Hayashi, M., Ohashi, N., Sunada, K., Hasegawa, T., & Fukui, Y. 1994, *Nature*, 368, 719
- Morton, D. C. 1974, *ApJ*, 193, L35
- Mouschovias, T. Ch., & Psaltis, D. 1995, *ApJ*, 444, L105
- Mouschovias, T. Ch., & Spitzer, L., Jr. 1976, *ApJ*, 210, 326
- Myers, P. C. 1978, *ApJ*, 225, 380
- . 1983, *ApJ*, 270, 105
- Myers, P. C., & Benson, P. J. 1983, *ApJ*, 266, 309
- Myers, P. C., Fuller, G. A., Goodman, A. A., & Benson, P. J. 1991, *ApJ*, 376, 561
- Myers, P. C., & Goodman, A. A. 1988, *ApJ*, 326, L27
- Myers, P. C., & Khersonsky, V. K. 1995, *ApJ*, 442, 186
- Myers, P. C., Linke, R. A., & Benson, P. J. 1983, *ApJ*, 264, 517
- Nakamura, F., Hanawa, T., & Nakano, T. 1995, *ApJ*, 444, 770
- Nakano, T. 1979, *PASJ*, 31, 697
- . 1981, *Prog. Theor. Phys. Suppl.*, 70, 54
- . 1982, *PASJ*, 34, 337
- . 1983, *PASJ*, 35, 209
- . 1984, *Fundam. Cosmic Phys.*, 9, 139
- . 1988, *PASJ*, 40, 593
- Nakano, T., Hasegawa, T., & Norman, C. 1995, *ApJ*, 450, 183
- Nakano, T., & Nakamura, T. 1978, *PASJ*, 30, 671
- Nakano, T., Nishi, R., & Umebayashi, T. 1996, in *The Role of Dust in the Formation of Stars*, ed. H. U. Käufel & R. Siebenmorgen (Berlin: Springer), 393
- Nakano, T., & Umebayashi, T. 1986, *MNRAS*, 218, 663
- Nishi, R., Nakano, T., & Umebayashi, T. 1991, *ApJ*, 368, 181
- Norman, C., & Silk, J. 1980, *ApJ*, 238, 158
- Ryden, B. S. 1996, *ApJ*, 471, 822
- Safer, P. N., McKee, C. F., & Stahler, S. W. 1997, *ApJ*, 485, 660
- Savage, B. D., & Mathis, J. S. 1979, *ARA&A*, 17, 73
- Scalo, J. M., & Pumphrey, W. A. 1982, *ApJ*, 258, L29
- Shu, F. H. 1977, *ApJ*, 214, 488
- Shu, F. H., Adams, F. C., & Lizano, S. 1987, *ARA&A*, 25, 23
- Simon, M., Chen, W. P., Howell, R. R., Benson, J. A., & Slowik, D. 1992, *ApJ*, 384, 212
- Spitzer, L., Jr. 1968, *Diffuse Matter in Space* (New York: Wiley)
- Strittmatter, P. A. 1966, *MNRAS*, 132, 359
- Tatematsu, K., et al. 1993, *ApJ*, 404, 643
- Tomisaka, K. 1996, *PASJ*, 48, L97
- Tomisaka, K., Ikeuchi, S., & Nakamura, T. 1988, *ApJ*, 335, 239
- . 1990, *ApJ*, 362, 202
- Umebayashi, T., & Nakano, T. 1990, *MNRAS*, 243, 103
- Ward-Thompson, D., Scott, P. F., Hills, R. E., & André, P. 1994, *MNRAS*, 268, 276
- Whittet, D. C. B., Bode, M. F., Longmore, A. J., Adamson, A. J., McFadzean, A. D., Aitken, D. K., & Roche, P. F. 1988, *MNRAS*, 233, 321
- Whitworth, A. P., Bhattal, A. S., Francis, N., & Watkins, S. J. 1996, *MNRAS*, 283, 1061
- Zweibel, E. G., & Josafatsson, K. 1983, *ApJ*, 270, 511